Reduction in Thrombotic Events With Heparin-Coated Palmaz-Schatz Stents in Normal Porcine Coronary Arteries*

Peter A. Hårdhammar, MD; Heleen M.M. van Beusekom, PhD; Håkan U. Emanuelsson, MD; Sjoerd H. Hofma, MD; Per A. Albertsson, MD; Pieter D. Verdouw, PhD; Eric Boersma, MSc; Patrick W. Serruys, MD, PhD; Willem J. van der Giessen, MD, PhD

Background The use of stents improves the result after balloon coronary angioplasty. Thrombogenicity of stents is, however, a concern. In the present study, we compared stents with an antithrombotic coating with regular stents.

Methods and Results Regular stents were placed in coronary arteries of pigs receiving no aspirin (group 1; n=8) or aspirin over 4 weeks (group 2, n=10) or 12 weeks (group 3, n=9). Stents coated with heparin (antithrombin III uptake, 5 pmol/stent) were placed in 7 pigs that did not receive aspirin (group 4). The other animals received aspirin and coated stents with a heparin activity of 12 pmol antithrombin III/stent (group 5, n=10) or 20 pmol/stent (group 6, n=10; group 7, n=10). Quantitative arteriography was performed at implantation and after 4 (groups 1, 2, and 4 through 6) or 12 weeks (groups 3 and 7). In an additional 5 animals, five regular and five coated stents (20 pmol/stent) were placed and explanted after 5 days for examination of the early responses to the implants. Thrombotic occlusion of the regular stent occurred in 9 of 27 in groups 1 through 3. However, in 0 of 30 of the animals receiving high-activity heparin-coated stents (groups 5 through 7), thrombotic stent occlusion was observed ($P<.001$). Histological analysis at 4 weeks showed that the neointima in group 6 was thicker compared with its control group 2 (259±104 and 117±36 μm, $P<.01$), but at 12 weeks the thickness was similar (152±61 and 198±49 μm, respectively). Comparison at 5 days suggested delayed endothelialization of the coating.

Conclusions High-activity heparin coating of stents eliminates subacute thrombosis in porcine coronary arteries. (*Circulation*. 1996;93:423-430.)

Key Words • stents • thrombosis • heparin

Over the past 15 years, the operator experience and equipment involved in PTCA have improved. Nevertheless, acute or subacute occlusion of the dilated artery occurs in 3% to 8% of cases within hours to days, requiring an immediate repeat procedure or emergency coronary bypass graft surgery.[1] Another unresolved issue of PTCA is late restenosis, which occurs in 30% to 50% of cases, predominantly after 3 to 6 months.[2,3] There is no effective pharmacological prevention of the restenosis process.[4-6]

Aspirin can reduce the incidence of acute occlusion to a limited extent.[7] High-dose systemic antiplatelet drug therapy may be more effective as it reduces early complications after PTCA by approximately 35%—at the expense, however, of more bleeding complications.[8] This beneficial effect appears to be sustained, as a reduction in the need for later revascularization has also been observed.[9]

The only proven approach to reduction of the incidence of late restenosis (by 25% to 31%) is the use of coronary stents.[10,11] The use of stents, however, is not free from complications because of the risk of stent thrombosis and bleeding or vascular complications, requiring both costly monitoring and a prolonged hospital stay.[10-19] Therefore, a combination of drugs and stents has been proposed to overcome both early and late complications of PTCA.[16-19]

Several approaches have been introduced to improve the surface properties of vascular prostheses.[20] Heparin coating of stents is an attractive method because the anticoagulant properties of heparin,[21] its inhibitory effect on mesenchymal cell growth and differentiation,[22-24] and extracellular matrix formation[25] are well established. The aim of the present study was to compare the thrombogenicity and histological features of stents with and without heparin coating after implantation in the coronary circulation in pigs.

Methods

Balloon-Expandable Intracoronary Stent

The stent used in the present study (Palmaz-Schatz coronary stent, Johnson & Johnson Interventional Systems Co) is composed of two segments (7 mm each) of slotted tubes connected by a short (1-mm) coupler, and it is mounted coaxially over the balloon of an angioplasty catheter.[26] When expanded, the metallic contact surface area is 10% to 15%.

Heparin Coating of Palmaz-Schatz Stent

The coating applied to the stents consists of heparin molecules that have been end point covalently coupled to an underlying polymer matrix (a modification of the CBAS[27] [Carmeda AB]). The efficacy of this coating is based on the continuous and repeated interaction between the active site of the immobilized heparin and circulating antithrombin III. The

Received August 14, 1995; revision received October 16, 1995; accepted October 18, 1995.

From the Department of Cardiology, Thoraxcenter, Erasmus University Rotterdam (The Netherlands), and Division of Cardiology, Sahlgrenska Hospital, Gothenburg, Sweden.

Correspondence to Willem J. van der Giessen, MD, Department of Cardiology, Thoraxcenter, Bd 412, Erasmus University Rotterdam, 3015 GD Rotterdam, The Netherlands.

*This manuscript is placed in "Clinical Investigations and Reports" so as to accompany the preceding manuscript.

Selected Abbreviations and Acronyms
CBAS = Carmeda Bioactive Surface
LAD = left anterior descending coronary artery
PTCA = percutaneous transluminal coronary angioplasty

coating consists, in principle, of four layers. A first layer on top of the steel is a polyamine layer; a dextran sulfate layer is applied on top of that. The third base layer is polyamine. Finally, these functional amino groups are covalently coupled to the aldehyde groups of partially degraded heparin molecules (Fig 1). The heparin activity of the coated stent is measured according to its ability to bind antithrombin III with high affinity and expressed in picomoles (of antithrombin III) per stent.

Approximately 15% of the end point–attached heparin molecules will carry the high-affinity antithrombin III–binding site, which is responsible for the anticoagulant action of the compound. Modifications of the surface chemistry and selection of heparin molecules with binding sites for antithrombin III were used to increase the antithrombin III–binding activity of three coatings of incremental activity (onefold to fourfold higher activity per surface area than the conventional CBAS). Pilot in vitro studies have shown that (1) mounting and expansion of the stent did not affect the integrity of the coating, as demonstrated with a colorimetric assay using toluidine blue[28]; and (2) sterilization with heat or ethylene oxide reduced the antithrombin III–binding activity considerably (50% to 70%). Consequently, the stents used in this study were initially coated under clean room conditions but not sterilized (group 4; Table 1); coated stents for later groups were sterilized and therefore initially coated with a higher heparin content to compensate for the loss during ethylene-oxide sterilization (groups 5 through 7). At the end of the study, the remaining heparin activity at the surface of explanted stents (both coated and controls) was assessed with the use of an antithrombin III–binding assay.

Animal Preparation

Experiments were performed in cross-bred Landrace-Yorkshire pigs (20 to 28 kg in weight; HVC) as described previously.[29] The investigations were carried out according to a protocol approved by the Committee on Experimental Animals of Erasmus University. After an overnight fast, the animals were sedated with 20 mg/kg ketamine hydrochloride. After endotracheal intubation, the pigs were connected to a ventilator that administered a mixture of oxygen and nitrous oxide (1:2, v/v). Anesthesia was maintained with 1 to 4 vol% enflurane. Antibiotic prophylaxis was administered by an intramuscular injection of 1000 mg of a mixture of procaine penicillin G and benzathine penicillin G. Under sterile conditions and after additional local anesthesia of the skin with lidocaine 2%, an arteriotomy of the left carotid artery was performed, and a 9F introduction sheath was placed. Heparin sodium (10 000 IU) was administered, and a 9F guiding catheter was advanced to the ascending aorta. After measurement of arterial blood pressure and heart rate and after withdrawal of an arterial blood sample for the measurement of blood gases and acid-base balance (settings of the ventilator were corrected if necessary), coronary angiography was performed with iopamidol (Iopamiro 370) as contrast agent. Seventy-eight animals underwent the catheterization procedures. Of these, 9 animals were excluded from final analysis due to the following reasons. In 3 animals, a stent was not implanted due to a coronary artery anomaly, air embolism at baseline angiography, and spontaneous arrhythmias, respectively. Complications during stent implantation (ventricular fibrillation or arrest during balloon inflation or balloon rupture) occurred in 3 other animals. Postoperative problems (aspiration hypoxia, reanesthesia for postoperative bleeding, and a leg problem) were the reason for premature withdrawal in 3 additional animals and were considered to be unrelated to stent placement.

Final analysis was performed for 69 animals, in which stent implantation was successful and no adverse events were observed.

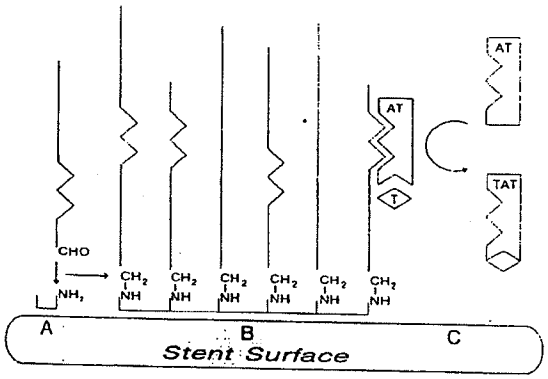

FIG 1. Principle of heparin coating and mechanism of antithrombotic action of heparin-coated stent surface. A, The metal surface has been conditioned with functional amino groups that can bind covalently with the aldehyde group of fragmented heparin molecules. B, Thus, end point–attached heparin molecules form a heterogeneous population, some without and some with the epsilon-shaped antithrombin III (AT)–binding region. C, Circulating antithrombin can bind to the active site, which catalyzes the inhibition of activated coagulation factors, eg, thrombin (T). The resultant inactive antithrombin/thrombin complex (TAT) is released into the bloodstream, thereby enabling the active site on the heparin to repeat interaction with AT and TAT.

TABLE 1. Experimental Groups, Treatment, and Size of Implanted Stents

Group	Stents, No. of Animals	Heparin, pmol/stent	Aspirin, 300 mg/d	Stent Size, 3.0/3.5/4.0 mm	Follow-up, wk
1	8	–	–	4/3/1	4
2	10	–	+	5/5/0	4
3	9	–	+	1/8/0	12
4	7	5	–	4/2/1	4
5	10	12	+	6/4/0	4
6	10	20	+	3/7/0	4
7	10	20	+	2/8/0	12

Stent Implantation

Based on the angiograms and with the diameter of the guiding catheter used as a reference, a segment with a diameter of 2.5 to 3.5 mm was selected in the proximal LAD using on-line quantitative coronary arteriography after intracoronary injection of 1 mg isosorbide dinitrate. Side branches were not avoided, but stents were not placed at curved coronary artery segments. Then, a heparin-coated or a regular stent (in alternate order) crimped on its deflated balloon was advanced over a 0.014-inch steerable guide wire to the preselected site for implantation. The balloon was inflated to a pressure of 6 atm for 30 seconds and then deflated, and negative pressure was maintained for 20 seconds. The catheter was then slowly withdrawn while leaving the stent in place. After repeat angiography of the stented coronary artery, the guiding catheter and the introducer sheath were removed, the arteriotomy was repaired, the skin was closed in two layers, and the animals were allowed to recover from anesthesia. Animals receiving the control stents and the three types of heparin-coated stents were assigned to seven groups (Table 1). Fifteen animals did not receive antithrombotic prophylaxis after the procedure (groups

1 and 4). Forty-nine animals received 300 mg acetylsalicylic acid/day PO, starting the day before implantation; this treatment was continued daily during the follow-up period.

Follow-up Angiography and Quantitative Analysis

The anesthesia and catheterization procedures at 4- or 12-week follow-up were similar, as described above; coronary angiography was performed in the same projection, and identical settings of the x-ray equipment were used during implantation. All coronary angiograms were measured on-line using a personal computer-based system for quantitative angiographic analysis with the edge-detection method (Cardiovascular Measurement System, Medis Inc).[30]

Microscopic Examination

After angiography at follow-up, the thorax was opened by a midsternal split, and a lethal dose of sodium pentobarbital was injected intravenously, immediately followed by cross-clamping of the ascending aorta. After the aortic root was punctured above the coronary ostia, 300 mL saline followed by 500 mL buffered 4% formaldehyde were infused under a pressure of 150 cm H_2O. The heart was then excised, and the coronary arteries were dissected from the epicardial surface. The stented and adjacent unstented segments were placed in 4% formaldehyde in phosphate buffer, pH 7.3, for at least 48 hours in preparation for microscopy. After further fixation for at least 48 hours, the tissue was processed for light microscopic examination as described previously.[29] Hematoxylin and eosin was used as a routine stain, and resorcin-fuchsin was used as an elastin stain.

Morphometry

For measurement of the thickness of the various layers of the arterial wall, at least six resorcin-fuchsin–stained sections of each stented coronary segment were examined from the proximal, mid, and distal portions of the stent. With a calibrated eyepiece, the neointimal and medial thicknesses were measured on top of and between the stent struts. The distance between the endothelial lining and the stent strut or internal elastic lamina was taken as the thickness of the intima.[31] The media was defined as the layer between the internal and external elastic laminae.

Assessment of Stent Thrombosis

Immediately after the animals were sacrificed and the arteries underwent fixation or after autopsy, the stented coronary artery was opened lengthwise using a pair of fine scissors and examined under a dissection microscope. Low-power photomicrographs were taken from each coronary artery, and the presence or absence of stent occlusion was assessed by two observers. In addition, light microscopical examination was used to confirm the thrombotic origin of the occlusion, as demonstrated by the presence of a platelet-rich, layered thrombus.

Assessment of the Early Response to Stent Implantation

In an additional group of five animals, one regular stent (in the left circumflex coronary artery) and one high-activity heparin-coated stent (in LAD) were placed per animal. These animals received procedural heparin during the implantation plus 300 mg acetylsalicylic acid during 5 days of follow-up. At 5 days, repeat angiography was performed, followed by excision of the stented coronary arteries for light microscopy and morphometry, as described. In addition, lectin cytochemistry and scanning electron microscopy were performed to study and compare the early blood and tissue responses to the regular and coated stents, by using previously described methods.[32]

TABLE 2. Experimental Groups, Outcome, and Size of Stents With Complications

Group	No. of Animals	Heparin Coating, pmol/stent	Stent Occlusion	Stent Size, mm
1	8	...	2	2×3.0
2	10	...	4	2×3.0
				2×3.5
3	9	...	3	3×3.5
4	7	5	3	3×3.0
5	10	12	0*	...
6	10	20	0*†	...
7	10	20	0*†	...

*$P<.001$ groups 5 through 7 vs groups 2 plus 3.
†$P\leq.01$ groups 6 plus 7 vs groups 2 plus 3.

Statistical Analysis

All data are expressed as mean±SD. The occurrence of thrombotic events between the groups was compared by Fisher's exact test. A two-tailed P value of $<.05$ was considered statistically significant. The significance of the changes in the angiographic and morphometric data were evaluated by unpaired t test when ANOVA indicated that the groups belonged to different populations. Because of repeated comparisons for these two parameters, only $P<.01$ (two-tailed) was considered statistically significant.

Results

Systemic Hemodynamics and Blood Gases During Angiography

During implantation, heart rate and mean arterial blood pressure were similar for all groups (99±14 beats per minute and 74±14 mm Hg, respectively). At restudy after 4 weeks (groups 1 through 5), heart rate (105±18 beats per minute) and mean arterial blood pressure (85±17 mm Hg) were comparable, but when restudied after 12 weeks, groups 6 and 7 showed an increase in these parameters (to 112±25 beats per minute and 101±22 mm Hg, respectively; $P<.01$). However, at no time was there any difference between the groups with coated or control stents. The oxygenation of arterial blood and acid-base balance were in the normal range during stent placement and follow-up angiography.

Follow-up Evaluation

In 64 animals, the stent could be placed successfully, and these were included in the final analysis. Eight of the animals that received a noncoated stent died suddenly within 48 hours, whereas a ninth pig survived 4 weeks with an infarction of the LAD perfused myocardium (Table 2).

In the animals receiving the 5 pmol/stent heparin coating without aspirin (group 4), three cases of sudden death occurred within 48 hours. However, all animals survived that received a stent with 12 or 20 pmol/stent heparin coating in combination with oral aspirin (groups 5 through 7). The data in Table 2 also show that problems were not associated with smaller-diameter stents.

Quantitative Angiographic Measurements

Quantitative analysis of the baseline coronary angiograms showed that luminal diameters of the proximal LAD were similar for all groups (range, 2.9 to 3.2 mm; Table 3). The diameters of the stent-mounted angioplasty balloons at maximal inflation pressure also did not

TABLE 3. Quantitative Angiographically Assessed Mean Diameters of Arteries and Balloon at the Site of Stent Implantation at Baseline, Immediately After Placement, and After 4 or 12 Weeks of Follow-up

Group	No. of Animals	Baseline, mm	Balloon, mm	Stent, mm	Follow-up 4 wk, mm	Follow-up 12 wk, mm
1	8	2.9±0.4	3.2±0.5	3.2±0.3	2.7±0.6	...
2	10	2.9±0.3	2.9±0.3	2.8±0.3	2.7±0.3	...
3	10	3.2±0.2	3.1±0.3	3.1±0.2	...	2.8±0.2
4	7	3.2±0.6	2.9±0.4	3.1±0.5	2.4±0.4	...
5	10	2.9±0.3	2.8±0.3	2.8±0.2	2.6±0.3	...
6	10	3.0±0.3	3.0±0.4	3.1±0.3*	2.4±0.4*	...
7	10	3.1±0.2	3.0±0.3	3.0±0.3	...	3.2±0.4†

Values are mean±SD.
*$P<.01$ vs group 2.
†$P<.01$ vs groups 3 and 6.

differ between the groups (range, 2.8 to 3.2 mm). The measured balloon-to-artery ratio was 1.0, demonstrating precise matching of balloons and recipient arteries. Implantation of the stents did not change the arterial diameters of the groups (range, 2.8 to 3.2 mm).

After 4 weeks of follow-up, the average luminal diameter showed no change in both control groups as well as in the groups receiving the low- or intermediate-activity heparin-coated stent. However, in the highest-activity heparin-coated stent group (group 6), the diameter had decreased by 0.7±0.6 mm ($P<.01$).

After 12 weeks of follow-up, the group receiving the control stents did not show a decrease in luminal diameter compared with the 4-week data for groups 1 and 3. However, the group receiving the high-activity coated stents (group 7) now showed no change in luminal diameter compared with its baseline and immediately poststent angiograms, and an actual increase occurred compared with the 4-week high-activity stented group.

Stent Thrombosis

On postmortem examination, all stents retrieved from animals that received a regular stent and died suddenly demonstrated stent occlusion (Fig 2A and 2B) in several cases accompanied by myocardial infarction of the corresponding anterior wall of the left ventricle. Major disruption of the vessel wall or incomplete expansion or marked overdilatation of the stent was not observed in these specimens. Microscopical examination confirmed the presence of a layered, platelet-rich thrombus in all occluded stents. In the group receiving the low-activity coated stents (group 4), all three cases of sudden death proved to be caused by stent thrombosis. In none of the animals receiving a stent with 12 or 20 pmol heparin/stent was partial or occlusive stent thrombosis observed.

Therefore, (sub)acute stent thrombosis was observed in 37% in the groups receiving regular noncoated stents ($P<.01$), and the only factor that could be identified as responsible for stent occlusion was the absence of the high-dose heparin coating.

Light Microscopy

Examination of the seven groups showed that all stents were covered by a neointima of variable thickness (Fig 3A through 3D), ranging from only several cell layers to a collagen- and elastin-rich tissue up to 500 μm in thickness. Typically, such a neointima contained a large amount of extracellular matrix with smooth muscle cells in disarray near the intimal/medial border. Toward the lumen, the tissue was more dense and cellular, containing macrophages and a few lymphocytes but mainly smooth muscle cells oriented in a circular fashion.

Medial impression by the stent struts was variable. Some metal struts lacerated only the internal elastic lamina. A minority of the struts, however, penetrated the medial layer, resulting in either a clean cut into the media or actual dissection, sometimes with damage to the external elastic lamina. Even in those cases, inflammatory changes were minimal and discrete (Fig 3). An active inflammatory reaction was rarely observed, and only in two (control stents) was a cellular response with

FIG 2. A, Photomacrograph of a control stent (group 3) occluded with a platelet-rich thrombus (arrow) causing sudden death approximately 27 hours after implantation. The stent has been opened longitudinally (arrowheads indicate struts). B, Photomicrograph of the thrombosed stent shown in A. Both the stent wire (* indicates stent wire void) and the luminal border are lined with a single layer of leukocytes (arrow). The lumen (L) is obstructed by a platelet-rich thrombus, showing the typical layered appearance (arrowhead) of an in vivo thrombotic occlusion. M indicates media; A, adventitia; E, erythrocytes; F, fibrin; and bar, 50 μm.

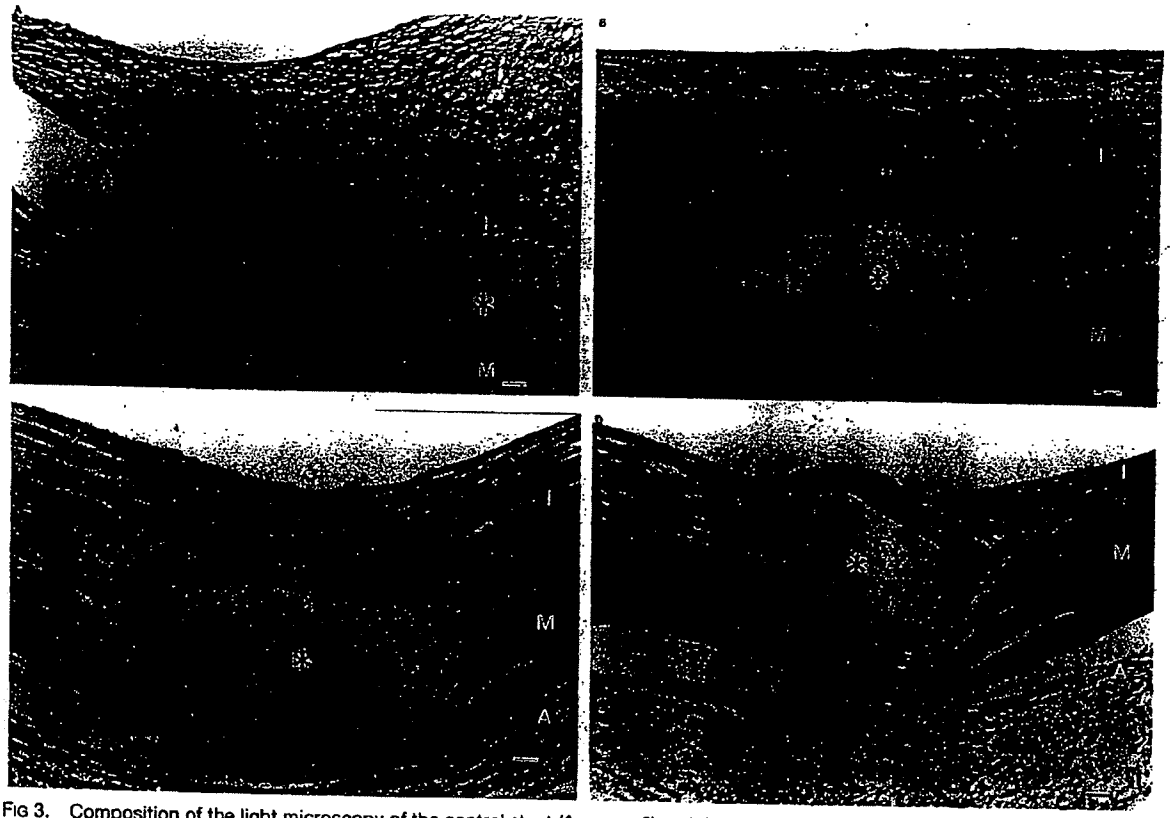

FIG 3. Composition of the light microscopy of the control stent (A, group 2) and the heparin-coated stent (B, group 6) at 4 weeks after implantation, and of the control stent (C, group 3) and the heparin-coated stent (D, group 7) at 12 weeks after implantation. In all specimens, the tissue response consisted of a neointimal thickness containing smooth muscle cells within a collagenous matrix. Although the thickness varied among the groups, the overall reaction was limited in its nature. I indicates intima; M, media; A, adventitia; *, stent wire void; and bar, 25 μm. Hematoxylin azophloxin stain.

monocytes and macrophages more prominently associated with the stents.

The only difference between the 4- and 12-week groups was an increase in neovascularization from adventitia toward the intima in the later group, in both coated and control stents. The only late features exclusively seen in some coated stents was an occasional spot of calcification (in two coated stents) and swollen appearance of the overlying endothelium (three coated stents).

Morphometry

Comparison after 4 weeks of follow-up showed that there was no difference in neointimal thickening between groups 1 and 4 (both received no aspirin after the procedure) and between groups 2 and 5 (Table 4). However, a comparison of groups 2 and 6 and of groups 5 and 6 showed that the increased thickening of the neointima in the group with the highest heparin activity was significant ($P<.01$). The thickness of the media under the metal struts did not differ between the groups.

After 12 weeks of follow-up, the difference between coated and noncoated stents was no longer observed as the thickness in the high-activity heparin-coated group was significantly smaller after 12 weeks (group 7) compared with at 4 weeks (group 6; $P<.01$). Along the length of the stent, from proximal to distal, there was an observed increase in intimal thickening for both the coated and the regular stent groups. The measurements

TABLE 4. Morphometry

Group	No. of Animals	NS, μm	N, μm	MS, μm	M, μm
1	6	263±93	301±127	120±66	195±58
2	6	117±36	100±43	90±19	156±16
3	6	198±49	185±33	110±26	187±20
4	4	166±35	175±30	90±13	174±45
5	10	109±55	98±51	90±21	154±26
6	10	259±104*	210±82	99±22	187±28
7	10	152±61	156±51	113±16	172±20

Values are mean±SD. NS indicates neointima covering stent struts; N, neointima between stent struts; MS, media under stent struts; and M, media between stent struts.
*$P<.01$ vs groups 2, 5, and 7.

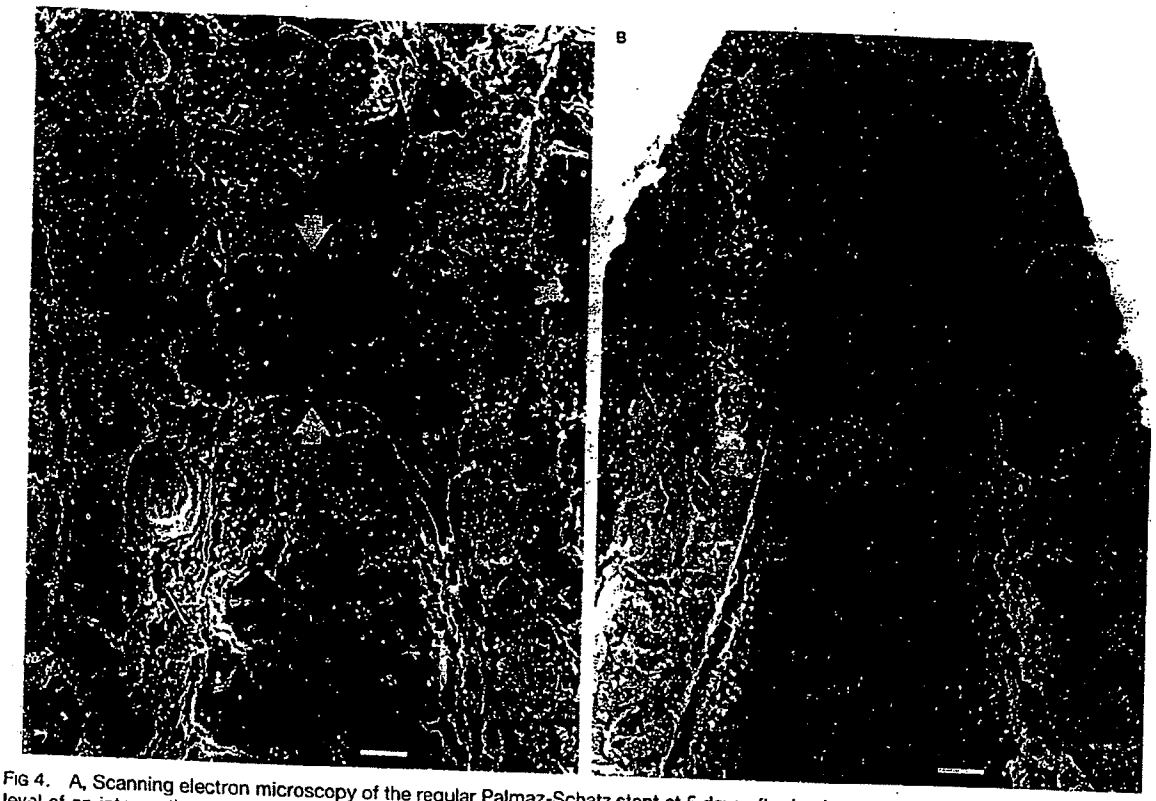

FIG 4. A, Scanning electron microscopy of the regular Palmaz-Schatz stent at 5 days after implantation. The photograph, taken at the level of an intersection between two stent struts (arrows), shows advanced endothelial covering but marked leukocyte adhesion. Bar indicates 57 μm. B, Scanning electron microscopy of the highest-activity heparin-coated Palmaz-Schatz stent at 5 days after implantation. The photograph, again taken at the intersection between two stent struts, clearly shows the absence of endothelial cells. Only a variable number of leukocytes and a protein layer cover the struts, whereas in-between the endothelial layer appears to be intact. Bar indicates 57 μm.

of other vessel wall layers did not differ between the groups.

Assessment of the Early Response to Stent Implantation

In the additional group of five animals, five coated stents (20 pmol antithrombin III uptake) and five regular stents were placed (balloon-to-artery ratio, 1.0±0.1). Angiographically measured coronary diameters before implantation, immediately after implantation, and after 5 days of follow-up for the heparin-coated stents were 2.9±0.2, 3.0±0.2, and 3.0±0.3 mm, respectively; and for the regular stents, diameters were 2.7±0.2, 2.9±0.2, and 2.8±0.5 mm, respectively (P=NS). Morphometrical assessment of the thickness of the layer covering the stent struts showed no differences between the two types of stents (57±17 μm for the heparin-coated stents and 62±47 μm for the regular stents). Light microscopy demonstrated that the early local reactions to both types of stent were similar, showing a proteinaceous adherent layer with adherent leukocytes. However, both the lectin cytochemical identification of endothelium and the scanning electron microscopy demonstrated a decreased endothelial cell covering of the heparin-coated stents (Fig 4A and 4B).

Heparin Activity of the Stents After Explantation

The control stents showed no detectable antithrombin III–binding activity after 4 weeks of follow-up (n=2). However, measurement of the coated stents explanted at the same time revealed that 20% to 50% of this activity was still detectable at 4 weeks (n=2).

Discussion

Metal Stents Reduce Restenosis but Are Thrombogenic

PTCA with balloon dilatation is a good alternative treatment to aortocoronary bypass surgery for patients with symptomatic coronary heart disease. Surgery offers longer symptomatic relief but is more invasive and requires a longer rehabilitation period.[33] PTCA allows patients to regain active life earlier, but in many patients the duration of symptomatic relief is shorter due to the restenosis process. Recently, two randomized clinical trials that compared balloon angioplasty with stent implantation were completed.[10,11] Both trials showed that stent implantation reduced the need of revascularization due to restenosis by approximately 30%. These new data will influence the choice of therapy in patients eligible for both surgery and PTCA.

The favorable outcome of stent implantation, however, has its price: a longer hospital stay and a 15% vascular complication rate, both caused by the use of an extensive anticoagulant regimen to prevent subacute thrombosis of the stent. Stent thrombosis has been recognized as a problem inherent to all metal stents in

animal experiments as well as in patients with coronary heart disease.[10-19,32,34-36]

Heparin Coating

Stents with improved surface characteristics may further enhance the clinical results of coronary stenting by reducing the risk of thrombotic stent occlusion. The same techniques that have been applied to improve the blood compatibility of vascular grafts may also enhance the quality of stents.[20] A widely used technique is coating of the cardiovascular implant surface with heparin.[37,38] In the present study, we tested an established heparin coating (CBAS)[27] and subsequent modifications of this coating applied the stainless steel Palmaz-Schatz coronary stent.

Reduction in Stent Thrombosis by High-Activity Heparin Coating

In the present study, the standard CBAS coating (5 pmol/stent) did not reduce the incidence of early thrombotic complications (Table 2). Subsequently, 300 mg aspirin was administered daily to the animals to reduce the background thrombogenicity in the animal stent model. The use of stents coated with higher heparin activity subsequently groups eliminated thrombotic events compared with a new appropriate control group also receiving aspirin. The incidence of stent thrombosis in the control groups (25% to 33%) in the present study is similar to that observed earlier with a self-expanding metallic stent in the same model.[35] This high incidence of stent thrombosis of regular stainless steel stents is not an artificial feature of this swine model. During the initial clinical experience with the Palmaz-Schatz stent, an 18% incidence of subacute closure was observed when warfarin or Coumadin treatment was withheld.[39] Very recently, it has been reported that noncoated slotted tube stents show a 42% thrombotic occlusion rate in the rabbit iliac model.[40]

We did not include an additional experimental group receiving the standard coating and aspirin. Therefore, we cannot exclude a significant contribution of the surface conditioning inner layers of the coating (to which the heparin molecules were attached) to the overall thromboresistance of the stent. However, evidence in favor of an active role for heparin may be provided by studies that showed that thrombin inhibitors reduced platelet and fibrinogen deposition during arterial injury or stent placement in the pig.[41,42] However, other studies have shown that coating metal stents with only a passive polymer layer also reduces local platelet deposition or thrombotic occlusion in experimental animals.[35,43,44] Nevertheless, the results of the present study are consistent with the antithrombotic action of the CBAS coating in extracorporeal systems.[45,46]

Effect of Heparin Coating on Neointimal Hyperplasia

Heparin has been shown to reduce smooth muscle cell proliferation, an important component of the restenosis process, in injured arteries of experimental animals.[22-24,47-49] This property of heparin may be unrelated to its anticoagulant effect.[23] In the present study, we did not observe a reduction in the thickness of the neointimal layer due to the heparin coating. On the contrary, a temporary increase occurred in the group with the highest activity of the coating. Results for the early-response (5-day) group of the present study showed delayed wound healing, which indicates that the well-known action of heparin to reduce endothelial cell attachment and growth[50] is most likely responsible for the reduced endothelial control of smooth muscle cell growth.

However, the increased neointimal response with the highest activity heparin coating at 4 weeks proved to be only temporary as after 12 weeks the tissue response was similar for coated and noncoated stents.

Conclusions

This study demonstrates that heparin coating of metal stents reduces thrombotic events associated with their deployment in normal coronary arteries of pigs. If confirmed in clinical studies, this coated stent may permit reduction in the systemic anticoagulation responsible for vascular complications and longer hospital stay.

Acknowledgments

This study was supported by Johnson & Johnson Interventional Systems, Warren, NJ. The authors thank Yvonne van der Helm and Deirdre Whelan for helping with the histological analysis. Rob van Bremen is acknowledged for expert technical assistance. We are grateful to Drs E. Scholander and J. Riesenfeld (Carmeda AB, Stockholm, Sweden) for measurement of the antithrombin III–binding activity of the explanted stents.

References

1. De Feyter PJ, Van den Brand M, Laarman GJ, Van Domburg R, Serruys PW, Suryapranata H. Acute coronary artery occlusion during and after percutaneous transluminal coronary angioplasty: frequency, prediction, clinical course, management, and follow-up. *Circulation*. 1991;83:927-936.
2. Serruys PW, Luijten HE, Beatt KJ, de Feyter PJ, van den Brand M, Reiber JHC, ter Katen HJ, van Es GA, Hugenholtz PG. Incidence of restenosis after successful coronary angioplasty: a time-related phenomenon. *Circulation*. 1988;77:361-371.
3. Nobuyoshi M, Kimura T, Nosaka H, Mioka S, Ueno K, Yokoi H, Hamasaki N, Horiuchi H, Ohishi H. Restenosis after successful percutaneous transluminal coronary angioplasty: serial angiographic follow-up of 229 patients. *J Am Coll Cardiol*. 1988;12:616-623.
4. Blackshear JL, O'Callaghan WG, Califf RM. Medical approaches to prevention of restenosis after coronary angioplasty. *J Am Coll Cardiol*. 1987;9:834-848.
5. Popma JJ, Califf RM, Topol EJ. Clinical trials of restenosis after coronary angioplasty. *Circulation*. 1991;84:1426-1436.
6. Hermans WRM, Rensing BJ, Strauss BH, Serruys PW. Prevention of restenosis after percutaneous transluminal coronary angioplasty: the search for a 'magic bullet.' *Am Heart J*. 1991;122:171-187.
7. Chesebro JH, Webster MWI, Reeder GS, Mock MB, Grill DE, Bailey KR, Steichen S, Fuster V. Coronary angioplasty: antiplatelet therapy reduces acute complications but not restenosis. *Circulation*. 1989;80(suppl II):II-64. Abstract.
8. The EPIC Investigators. Use of a monoclonal antibody directed against the platelet glycoprotein IIb/IIIa receptor in high-risk coronary angioplasty. *N Engl J Med*. 1994;330:956-961.
9. Topol EJ, Califf RM, Weisman HF, Ellis SG, Tcheng JE, Worley S, Ivanhoe R, George BS, Fintel D, Weston M, Sigmon K, Anderson KM, Lee KL, Willerson JT, on behalf of the EPIC Investigators. Randomised trial of coronary intervention with antibody against platelet IIb/IIIa integrin for reduction of clinical restenosis: results at six months. *Lancet*. 1994;343:881-886.
10. Serruys PW, de Jaegere P, Kiemeneij F, Macaya C, Rutsch W, Heyndrickx G, Emanuelsson H, Marco J, Legrand V, Materne P, Belardi J, Sigwart U, Colombo A, Goy JJ, van den Heuvel P, Delcan J, Morel M, for the Benestent Study Group. A comparison of balloon expandable stent implantation with balloon angioplasty in patients with coronary artery disease. *N Engl J Med*. 1994;331:489-495.

11. Fishman DL, Leon MB, Baim DS, Schatz RA, Savage MP, Penn I, Detre K, Veltri L, Ricci D, Nobuyoshi M, Cleman M, Heuser R, Almond D, Teirstein PS, Fish RD, Colombo A, Brinker J, Moses J, Shaknovich A, Hirshfeld J, Bailey S, Ellis S, Rake R, Goldberg S, for the Stent Restenosis Study Investigators. A randomized comparison of coronary stent placement and balloon angioplasty in the treatment of coronary artery disease. *N Engl J Med*. 1994;331: 496-501.
12. Sigwart U, Puel J, Mirkovitch V, Joffre F, Kappenberger L. Intravascular stents to prevent occlusion and restenosis after transluminal angioplasty. *N Engl J Med*. 1987;316:701-706.
13. Serruys PW, Strauss BH, Beatt KJ, Bertrand ME, Puel J, Rickards AF, Meier B, Goy J-J, Vogt P, Kappenberger L, Sigwart U. Angiographic follow-up after placement of a self-expanding coronary stent. *N Engl J Med*. 1991;324:13-17.
14. Bucx JJJ, De Scheerder I, Beatt K, van den Brand M, Suryapranata H, de Feyter PJ, Serruys PW. The importance of adequate anticoagulation to prevent early thrombosis after stenting of stenosed venous bypass grafts. *Am Heart J*. 1991;121:1389-1396.
15. Moscucci M, Mansour KA, Kent KC, Kuntz RE, Senerchia C, Baim DS, Carrozza JP. Peripheral vascular complications of directional coronary atherectomy and stenting: predictors, management, and outcome. *Am J Cardiol*. 1994;74:448-453.
16. King SB III. Vascular stents and atherosclerosis. *Circulation*. 1989; 79:460-462.
17. Serruys PW, Beatt KJ, van der Giessen WJ. Stenting of coronary arteries: are we the sorcerer's apprentice? *Eur Heart J*. 1989;10: 774-782.
18. Serruys PW, Strauss BH, van Beusekom HMM, van der Giessen WJ. Stenting of coronary arteries: has a modern Pandora's box been opened? *J Am Coll Cardiol*. 1991;17(suppl B):143B-154B.
19. Topol EJ. Caveats about elective coronary stenting. *N Engl J Med*. 1994;331:539-541.
20. Hoffman AS. Modification of material surfaces to affect how they interact with blood. *Ann N Y Acad Sci*. 1987;516:96-101.
21. Hirsh J. Heparin. *N Engl J Med*. 1991;324:1565-1574.
22. Clowes AW, Karnovsky MJ. Suppression by heparin of smooth muscle cell proliferation in injured arteries. *Nature*. 1977;265: 625-626.
23. Guyton JR, Rosenberg RD, Clowes AW, Karnovsky MJ. Inhibition of rat arterial smooth muscle cell proliferation by heparin: in vivo studies with anticoagulant and nonanticoagulant heparin. *Circ Res*. 1980;46:625-634.
24. Edelman ER, Karnovsky MJ. Contrasting effects of the intermittent and continuous administration of heparin in experimental restenosis. *Circulation*. 1994;89:770-776.
25. Ofosu FA, Danishefsky I, Hirsh J. Heparin and related polysaccharides: structure and function. *Ann N Y Acad Sci*. 1989;556:1-501.
26. Schatz RA, Palmaz JC, Tio FC, Garcia F, Garcia O, Reuter SR. Balloon-expandable intracoronary stents in the adult dog. *Circulation*. 1987;76:450-457.
27. Larm O, Larsson R, Olsson P. A new non-thrombogenic surface prepared by selective covalent binding of heparin via a modified, reducing terminal residue. *Biomat Med Art Org*. 1983;11:161-173.
28. Shankar H, Senatore F, Wu DR, Avantsa S. Coimmobilization and interaction of heparin and plasmin on collageno-elastic tubes. *Biomat Art Cells Art Org*. 1990;18:59-73.
29. Van der Giessen WJ, Serruys PW, Van Beusekom HMM, van Woerkens LJ, van Loon H, Soei LK, Strauss BH, Beatt KJ, Verdouw PD. Coronary stenting with a new, radiopaque, balloon-expandable endoprosthesis in pigs. *Circulation*. 1991;83:1788-1798.
30. Reiber JHC, Serruys PW, Kooijman CJ, Wijns W, Slager CJ, Gerbrands JJ, Schuurbiers JCH, den Boer A, Hugenholtz PG. Assessment of short-, medium- and long-term variations in arterial dimensions from computer-assisted quantitation of coronary cineangiograms. *Circulation*. 1985;71:280-288.
31. Polimeni PI, Cunningham P, Otten MD, McCrea D. Morphometric quantification of atherosclerotic plaques by computer-assisted image-analysis of histographs. *Comput Biomed Res*. 1987;20: 113-124.
32. Van der Giessen WJ, van Beusekom HMM, van Houten CD, van Woerkens LJ, Verdouw PD, Serruys PW. Coronary stenting with polymer-coated and uncoated self-expanding endoprosthesis in pigs. *Coron Artery Dis*. 1992;3:631-640.
33. RITA Trial Participants. Coronary angioplasty versus coronary artery bypass surgery: the Randomised Intervention Treatment of Angina (RITA) trial. *Lancet*. 1993;341:573-580.
34. Rodgers GP, Minor ST, Robinson K, Cromeens D, Woolbert SC, Stevens LC, Guyton JR, Wright K, Roubin GS, Raizner AE. Adjuvant therapy for intracoronary stents: investigations in atherosclerotic swine. *Circulation*. 1990;82:560-569.
35. Krupski WC, Bass A, Kelly AB, Marzec UM, Hanson SR, Harker LA. Heparin-resistant thrombus formation by endovascular stents in baboons: interruption by a synthetic antithrombin. *Circulation*. 1990;82:570-577.
36. Roubin GS, Cannon AD, Agrawal SK, Macander PJ, Dean LS, Baxley WA, Breland J. Intracoronary stenting for acute and threatened closure complicating percutaneous transluminal coronary angioplasty. *Circulation*. 1992;85:916-927.
37. Olsson P, Larm O. Biologically active heparin coating in medical devices. *Int J Artif Organs*. 1991;14:453-456.
38. Engbers GH, Feijen J. Current techniques to improve the blood compatibility of biomaterial surfaces. *Int J Artif Organs*. 1991;14: 199-215.
39. Schatz RA, Baim DS, Leon M, Ellis SG, Goldberg S, Hirshfeld JW, Cleman MW, Cabin HS, Walker C, Stagg J, Buchbinder M, Teirstein PS, Topol EJ, Savage M, Perez JA, Curry RC, Whitworth H, Sousa E, Tio F, Almagor Y, Ponder R, Penn IM, Leonard B, Levine SL, Fish RD, Palmaz JC. Clinical experience with the Palmaz-Schatz coronary stent: initial results of a multicenter study. *Circulation*. 1991;83:148-161.
40. Rogers C, Edelman ER. Endovascular stent design dictates experimental restenosis and thrombosis. *Circulation*. 1995;91:2995-3001.
41. Heras M, Chesebro JH, Webster MWI, Mruk JS, Grill DE, Penny WJ, Bowie EJW, Badimon L, Fuster V. Hirudin, heparin, and placebo during deep arterial injury in the pig: the in vivo role of thrombin in platelet initiated thrombosis. *Circulation*. 1990;82: 1476-1484.
42. Buchwald AB, Sandrock D, Unterberg C, Ebbecke M, Nebendahl K, Lüders S, Munz DL, Wiegand V. Platelet and fibrin deposition on coronary stents in minipigs: effect of hirudin versus heparin. *J Am Coll Cardiol*. 1993;21:249-254.
43. Bailey SR, Guy DM, Garcia OJ, Paige S, Palmaz JC, Miller DD. Polymer coating of Palmaz-Schatz stent attenuates vascular spasm after stent placement. *Circulation*. 1990;82(suppl III):III-541. Abstract.
44. Whiffen JD, Young WP, Gott VL. Stability of the thrombus-resistant graphite-benzalkonium-heparin surface in an anti-heparin environment. *J Thorac Cardiovasc Surg*. 1964;48:317-322.
45. Videm V, Mollness TE, Garred P, Aasen AO, Svennevig JL. Biocompatibility of extracorporeal circulation: in vitro comparison of heparin coated and uncoated oxygenator circuits. *J Thorac Cardiovasc Surg*. 1991;101:654-660.
46. Von Segesser LK, Wiess BM, Leskosek B, Turina MI. Ventricular assist with heparin surface coated devices. *ASAIO Trans*. 1991;37: 278-279.
47. Edelman ER, Adams DH, Karnovsky MJ. Effect of controlled adventitial heparin delivery on smooth muscle cell proliferation following endothelial injury. *Proc Natl Acad Sci USA*. 1990;87: 3773-3777.
48. Hanke H, Oberhoff M, Hanke S, Hassenstein S, Kamenz J, Schmid KM, Betz E, Karsch KR. Inhibition of cellular proliferation after experimental balloon angioplasty by low-molecular-weight heparin. *Circulation*. 1992;85:1548-1556.
49. Buchwald A, Unterberg C, Nebendahl K, Grone H-J, Wiegand V. Low-molecular-weight heparin reduces neointimal proliferation after coronary stent implantation in hypercholesterolemic minipigs. *Circulation*. 1992;86:531-537.
50. Folkman J, Langer R, Lindhardt RJ, Haudenschild C, Taylor S. Angiogenesis inhibition and tumor regression caused by heparin or a heparin fragment in the presence of cortisone. *Science*. 1983;221: 719-725.

Topics in Applied Chemistry

Fluoropolymers 2

Properties

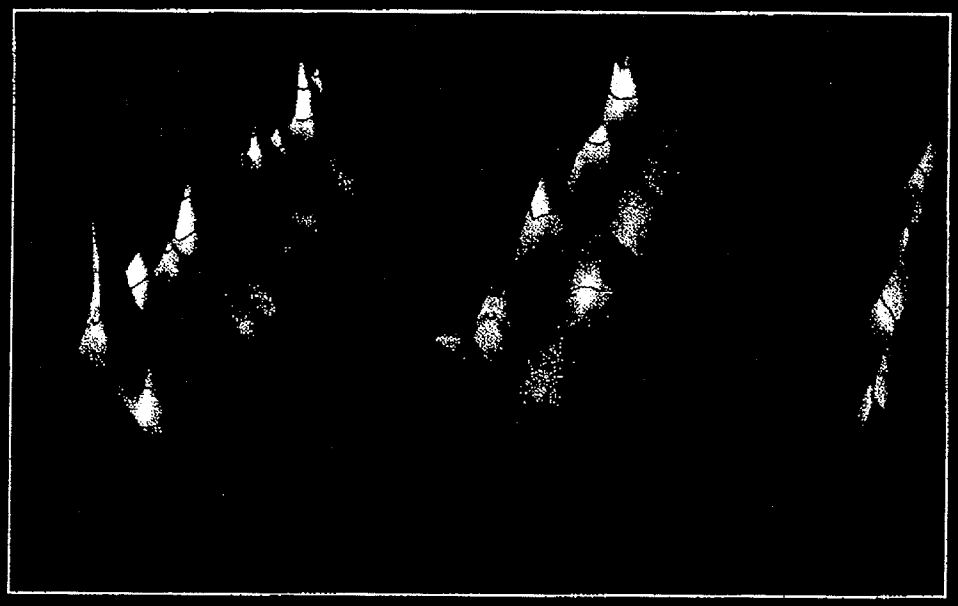

Edited by

Gareth Hougham, Patrick E. Cassidy, Ken Johns, and Theodore Davidson

TOPICS IN APPLIED CHEMISTRY

Series Editor: Alan R. Katritzky, FPS
University of Florida
Gainesville, Florida

Gebran J. Sabongi
3M Company
St. Paul, Minnesota

Current volumes in the series:

ANALYSIS AND DEFORMATION OF POLYMERIC MATERIALS
Paints, Plastics, Adhesives, and Inks
Jan W. Gooch

CHEMISTRY AND APPLICATIONS OF LEUCO DYES
Edited by Ramaiah Muthyala

FLUOROPOLYMERS 1: Synthesis
FLUOROPOLYMERS 2: Properties
Edited by Gareth Hougham, Patrick E. Cassidy, Ken Johns, and Theodore Davidson

FROM CHEMICAL TOPOLOGY TO THREE-DIMENSIONAL GEOMETRY
Edited by Alexandru T. Balaban

LEAD-BASED PAINT HANDBOOK
Jan W. Gooch

ORGANIC PHOTOCHROMIC AND THERMOCHROMIC COMPOUNDS
Volume 1: Main Photochromic Families
Volume 2: Physicochemical Studies, Biological Applications, and Thermochromism
Edited by John C. Crano and Robert J. Guglielmetti

ORGANOFLUORINE CHEMISTRY
Principles and Commercial Applications
Edited by R. E. Banks, B. E. Smart, and J. C. Tatlow

PHOSPHATE FIBERS
Edward J. Griffith

RESORCINOL
Its Uses and Derivatives
Hans Dressler

A Continuation Order Plan is available for this series. A continuation order will bring delivery of each new volume immediately upon publication. Volumes are billed only upon actual shipment. For further information please contact the publisher.

Fluoropolymers 2
Properties

Edited by

Gareth Hougham
IBM T. J. Watson Research Center
Yorktown Heights, New York

Patrick E. Cassidy
Southwest Texas State University
San Marcos, Texas

Ken Johns
Chemical and Polymer
Windlesham, Surrey, England

Theodore Davidson
Princeton, New Jersey

Kluwer Academic / Plenum Publishers
New York • Boston • Dordrecht • London • Moscow

Library of Congress Cataloging-in-Publication Data

Fluoropolymers / edited by Gareth Hougham ... [et al.].
p. cm. -- (Topics in applied chemistry)
Includes bibliographical references and indexes.
Contents: 1. Synthesis -- 2. Properties.
ISBN 0-306-46060-2 (v. 1). -- ISBN 0-306-46061-0 (v. 2)
1. Fluoropolymers. I. Hougham, Gareth. II. Series.
QD383.F48F54 1999
547'.70459--dc21 99-23732
CIP

Cover graphic: Conformational energy surface of 6FDA-PFMB fluorinated polyimide. Used to test correspondence between experimental activation energy of b transition and energy of rotation about phenyl-imide bond. [G. Hougham and T. Jackman, Polymer Preprints 37(1), 1996.] Graphic by G. Hougham and T. Jackman.

ISBN: 0-306-46061-0

233 Spring Street, New York, N.Y. 10013

10 9 8 7 6 5 4 3 2 1

A C.I.P. record of this book is available from the Library of Congress.

Printed in the United States of America

Contributors

Shinji Ando, Science and Core Technology Group, Nippon Telegraph and Telephone Corp. Musashino-shi, Tokyo 180, Japan. Present address: Department of Polymer Chemistry, Tokyo Institute of Technology, Meguro-ku, Tokyo 152, Japan

Karol Argasinski, Ausimont USA, Thorofare, New Jersey 08086

S. V. Babu, Department of Chemical Engineering, Clarkson University, Potsdam, New York 13699

Warren H. Buck, Ausimont USA, Thorofare, New Jersey 08086

Jeffrey D. Carbeck, Department of Chemical Engineering, Massachusetts Institute of Technology, Cambridge, Massachusetts 02139. Present address: Department of Chemical Engineering, Princeton University, Princeton, New Jersey 08544

Stephen Z. D. Cheng, Maurice Morton Institute and Department of Polymer Science, University of Akron, Akron, Ohio 44325-3909

Theodore Davidson, 109 Poe Road, Princeton, New Jersey 08540

C. R. Davis, IBM, Microelectronics Division, Hopewell Junction, New York 12533

Ronald K. Eby, Institute of Polymer Science, University of Akron, Akron, Ohio 44325

56. P. R. Herman, B. Chen, and D. J. Moore, in *Laser Ablation in Materials Processing: Fundamentals and Applications* (B. Braren, J. J. Dubowksi, and D. P. Norton, eds.), Materials Research Society, Pittsburgh (1992), Proc. 285.
57. F. D Egitto and C. R. Davis, *Appl. Phys. B55*, 488–493 (1992).
58. D. L. Singleton, G. Paraskevopoulos, and R. S. Taylor, *Chem. Phys. 144*, 415–423 (1990).
59. R. Taylor, D. L. Singleton, and G. Paraskevopoulos, *Appl. Phys. Lett. 50*(25), 1779–1781 (1987).
60. R. Srinivasan and B. Braren, *Chem. Rev. 89*(6), 1303–1316 (1989).
61. R. Srinivasan, B. Braren, and K. G. Casey, *Pure Appl. Chem. 62*(8), 1581–1584 (1990).
62. R. Linsker, R. Srinivasan, J. J. Wynne, and D. R. Alonso, *Lasers Surg. Med. 4*, 201–206 (1984).
63. S. R. Cain, C. E. Otis, and F. C. Burns, *J. Appl. Phys. 71*(9), 4107–4117 (1992).
64. V. Srinivasan, M. A. Smrtic, and S. V. Babu, *J. Appl. Phys. 59*(11), 3861–3867 (1986).
65. S. V. Babu, G. C. D'Couto, and F. D. Egitto, *J. Appl. Phys. 72*(2), 692–698 (1992).
66. H. Hiraoka, T. J. Chuang, and H. Masuhara, *J. Vac. Sci. Technol. B6*(1), 463–465 (1988).
67. R. Srinivasan and B. Braren, *Appl. Phys. A45*, 289–292 (1988).
68. T. J. Chuang, H. Hiraoka, and A. Modl, *Appl. Phys. A45*(4), 277–288 (1988).
69. W. W. Simons (ed.), *The Sadtler Handbook of Ultraviolet Spectra*, Sadtler Research Laboratories, Philadelphia (1979), p. 36.
70. F. D. Egitto and C. R. Davis, unpublished results (1993).
71. R. M. Silverstein, G. C. Bassler, and T. C. Morrill, *Spectrometric Identification of Organic Compounds, 4th Ed.*, John Wiley and Sons, New York (1981), p. 305.
72. C. R. Davis, F. D. Egitto, and S. L. Buchwalter, *Appl. Phys. B54*, 227–230 (1992).
73. D. H. Napper, *Polymeric Stabilization of Colloidal Dispersions*, Academic Press, New York (1993).
74. C. R. Davis and J. A. Zimmerman, *J. Appl. Polym. Sci. 54*, 153–162 (1994).
75. N. J. Turro, *Molecular Photochemistry*, Benjamin, New York (1965).
76. H. S. Cole, Y. S. Liu, and H. R. Philipp, *Appl. Phys. Lett. 48*(1), 76–77 (1986).
77. M. Bolle, K. Luther, J. Troe, J. Ihlemann, and H. Gerhardt, *Appl. Surf. Sci. 46*, 279–283 (1990).
78. G. C. D'Couto, S. V. Babu, F. D. Egitto, and C. R. Davis, *J. Appl. Phys. 74*(10), 5972–5980 (1993).
79. N. P. Furzikov, *Appl. Phys. Lett. 56*(17), 1638–1640 (1990).
80. G. C. D'Couto and S. V. Babu, *J. Appl. Phys. 76*(5), 3052–3058 (1994).
81. C. R. Davis, R. W. Snyder, F. D. Egitto, G. C. D'Couto, and S. V. Babu, *J. Appl. Phys. 76*(5), 3049–3051 (1994).
82. C. R. Davis and F. D. Egitto, *Polym. Mat. Sci. Eng. 66*, 257–258 (1992).

6

Novel Solvent and Dispersant Systems for Fluoropolymers and Silicones*

MARK W. GRENFELL

6.1. INTRODUCTION

Prior to their current phase-out, chlorofluorocarbons (CFCs) were widely used as processing solvents for various materials. CFCs were well suited for many medical applications owing to their high solvency, nonflammability, good materials compatibility, and low toxicity. The uses for CFCs include a silicone deposition solvent, a fluoropolymer dispersion liquid, and processing solvents. However, the Montreal Protocol phase-out of ozone-depleting substances has required that alternative dispersants and solvents be found. Limitations of most available alternatives include flammability, low volatility, poor solvency, and poor materials compatibility.

Perfluorocarbons (PFCs) have many functional properties that are similar to those of CFCs but they do not cause ozone depletion. Therefore they can be excellent replacements for CFCs in many demanding, high-performance applications. In addition to being non-ozone-depleting, PFCs are essentially nontoxic, nonflammable, nonvolatile organic compounds, easily dried, and available in a wide range of boiling points, and they provide excellent materials compatibility. Although PFCs exhibit poor solubility with most compounds, their ability to dissolve or disperse halogenated compounds is excellent. In addition, these

MARK W. GRENFELL · 3M Company, St. Paul, Minnesota 55144-1000

Fluoropolymers 2: Properties, edited by Hougham *et al.* Plenum Press, New York, 1999.

materials are easily recovered during use. Therefore, PFCs are ideally suited as bearer media for fluoropolymers, and when combined with cosolvents, they are useful as silicone solvents.

This chapter will discuss the advantageous properties of PFCs for use as carrier solvents and dispersants, and several application examples will be illustrated to demonstrate their efficacious use.

6.2. PERFLUOROCARBONS AND THEIR ADVANTAGES

Perfluorocarbons are a class of organic compounds in which all of the hydrogen atoms are replaced with fluorine atoms. They possess unique properties that make them very useful as dispersants, carrier solvents, and processing solvent additives. Their lack of chlorine or bromine atoms results in zero-ozone-depletion potential.

The strength of the carbon–fluorine bond results in a high degree of thermal and chemical stability, and in the extremely low toxicity of many perfluorinated compounds. Owing to their nonpolar structure, PFCs have excellent compatibility with nearly any substrate, including most plastics, elastomers, and metals, and because of their benign effect on plastics, they are very useful as additives to materials that act aggressively on polymeric substrates. For example, PFCs can be added to hydrochlorofluorocarbons (HCFCs) to reduce or eliminate the solvent attack of HCFCs on plastics. For coating operations, PFCs have a very low surface tension, which makes them effective wetting agents, and because of their low water solubility they are extremely useful in avoiding water contamination and water-supported bioburden. Owing to their nonflammability, PFCs can be used safely and do not require any special equipment or precautions. Table 6.1 lists the physical properties of several perfluorocarbons.[1]

6.3. FLUOROPOLYMER DISPERSIONS

Fluoropolymers, such as polytetrafluoroethylene (PTFE), are available in many product configurations, from powders to dispersions, and with a wide range of available features, such as various particle sizes, several molecular weights, and in some cases FDA approval. Fluoropolymers such as Teflon® and Vydax® are used extensively as dry lubricants, protective coatings, and release agents.[2,3]

Powdered PTFE is easily dispersed directly into PFCs and the dispersion can be applied to a substrate using dip-coating, spraying, painting, and spin-coating. Agitation is required to maintain a homogeneous dispersion.

Some PTFE products are supplied as dispersions. Prior to the phase-out of CFCs, Vydax® was used as a dispersion of solid PTFE in Freon®-113 (1,1,2-trichloro-1,2,2-trifluoroethane). The dispersions were often further diluted by the end user to meet individual process requirements. To replace Freon®-113, DuPont began supplying Vydax® in dispersions of isopropyl alcohol (IPA) and water. Several disadvantages are associated with these replacements. Both IPA and water are considerably less volatile than the previously employed CFCs. Therefore, coating homogeneity has suffered for many users. IPA dispersions are flammable, requiring additional precautions and capital equipment modifications. Water dispersions combine energy-inefficient drying and substrate corrosion as potential concerns to the user.

Table 6.1. Typical Physical Property Comparison of 3M Performance Fluids

Property	Typical values				
Chemical formula	C_5F_{12}	$C_5F_{11}NO$	C_6F_{14}	C_7F_{16}	C_8F_{18}
Commercial name	PF-5050	PF-5052	PF-5060	PF-5070	PF-5080
Average molecular weight	288	299	338	388	438
ODP (ozone depletion potential)	0.00	0.00	0.00	0.00	0.00
Boiling point (°C)	30	50	56	80	101
Liquid density (g/ml @ 25°C)	1.63	1.70	1.68	1.73	1.77
Liquid viscosity (cp @ 25°C)	0.65	0.68	0.68	0.95	1.4
Surface tension (dyn/cm @ 25°C)	9.5	13	12	13	14
Heat of vaporization (cal/g @ boiling point)	21	25	21	19	22
Vapor pressure (mm Hg @ 25°C)	610	274	232	79	29
Thermal conductivity					
Liquid (mW/m) · (K) @ 25°C)	56	62	57	60	64
Vapor (mW/m) · (K) @ 25°C	12.4	10.1	12.4	NA	NA
Solubility of H_2O (ppm by wt @ 25°C)	7	14	10	11	14
Solubility of fluorocarbons	High	High	High	High	High
Hildebrand solubility parameter $[H = (\text{cal/cm}^3)^{1/2}]$	5.5	6.3	5.6	5.7	5.7
Flash point (°C)	None	None	None	None	None

Low heats of vaporization and vapor pressures higher than IPA and water combine to provide PFCs with excellent evaporative characteristics. Differing volatilities available for PFCs and their mixtures allow the user to select a volatility for given process conditions. Therefore, PFCs used in coating are more easily evaporated from coated surfaces than water or IPA. Table 6.2 compares the relative evaporative properties of PFCs, IPA, and water. However, the boiling point of the mixture should be selected to minimize losses. By reducing losses and containing PFC emissions, process economics improve and environmental emissions of PFCs are lessened. When recovering the materials via condensation, the low heat of vaporization requires less energy to condense vaporized materials and their low solubilities with water and organics allow for easy separation of the recovered PFCs. The higher molecular weights of the PFCs

Table 6.2. Evaporative Properties of Various Fluoropolymer Dispersants

Solvent	Boiling point (°C)	Vapor pressure (mm Hg)	Heat of vaporization (cal/g at boiling point)
Perfluoro-*N*-methylmorpholine	50	274	25
Perfluorohexane	56	232	21
Perfluoroheptane	80	79	19
Isopropyl alcohol	82	43	131
Water	100	24	583

as compared to IPA and water result in lower diffusive losses from usage tanks for manufacturing processes. Additionally, PFCs can be recycled by distillation at the customer site or via 3M (see the Section 6.7 for additional details on recovering PFCs).

Although PFCs exhibit limited solubility with organic solvents, they can be used as diluents for PTFE dispersions such as Vydax® by introducing cosolvents. The HCFCs constitute a family of very effective cosolvents. HCFCs such as HCFC-141b (1,1-dichloro-1-fluoroethane) or HCFC-225 (pentafluorodichloropropane) bridge the gap between the solubilities of PFCs and organic solvents, enabling PFCs to be used with existing PTFE dispersion products. Employing PFCs as the diluent for Vydax® dispersions provides numerous advantages. PFCs are available in a wide range of boiling points, thus the volatility of the final coating solution can be optimized to required process conditions. The use of a PFC will normally eliminate the flammability of the limited quantity of the organic solvent, e.g., IPA, in use and will provide excellent materials compatibility with nearly all substrates.

A Vydax® AR/IPA dispersion that has the above beneficial properties can be prepared as follows: Vydax® AR/IPA is normally supplied from the manufacturer as a 30 wt % solid dispersion of PTFE in 70 wt % IPA. To create a 100-g sample of a 1 wt % solid dispersion suitable for coating, the proportions in Table 6.3

Table 6.3. Recipe to Create a 1 wt % Fluoropolymer Dispersion

Mixture component	Mass added on a 100-g basis (g)
Vydax® AR/IPA dispersion (Yielding 1.0 g PTFE and 2.33 g IPA)	3.3
HCFC-141b	27–30
PFC (e.g., perfluorohexane)	66.7–69.7

would be used. The dispersion can be easily maintained using agitation, and this dispersion system has proven useful for coating medical instruments with PTFE.

6.4. AMORPHOUS FLUOROPOLYMER SOLVENTS

Perfluorocarbons are the preferred solvent for amorphous fluoropolymers composed of tetrafluoroethylene (TFE) and 2,2-bistrifluoromethyl-4,5-difluoro-1,3-dioxole (PDD), such as Teflon AF®. Amorphous fluoropolymers exhibit many useful properties, such as high temperature stability, excellent chemical resistance, low water absorption, high light transmission, very low refractive index, and very low dielectric constant.[4] Amorphous copolymers dissolve into PFCs, creating solutions rather than the aforementioned dispersions. Solution behavior allows the polymers to be processed in a variety of ways. For example, the materials can be spin-coated, dip-coated, sprayed, or painted. Coating thicknesses can then be controlled by controlling solution concentrations. Additional coating thickness control is available by altering the withdrawal rate of coated objects in dip-coating operations.[5]

The solubility of Teflon AF® in perfluorinated compounds was presented by Buck and Resnick.[5] Table 6.4 lists several perfluorinated solvents in order of boiling point. The solubility parameters were calculated from the Small group contribution tables using a value of 100 for the group contribution of a CF group.

Table 6.4. Perfluorinated Solvents for Teflon® AF[5]

Solvent	Solubility parameter		
	BP (°C)	$(J/m^3)^{1/2}$	$(cal/cm^3)^{1/2}$ [a]
Perfluorohexane	60	0.0123	6.0
Perfluoromethylcyclohexane	76	0.0129	6.3
Perfluorobenzene	82	0.0123	6.0
Perfluorodimethylcyclohexane	102	0.0139	6.8
Perfluorooctane	103	0.0129	6.3
Perfluorodecalin	142	0.0135	6.6
Perfluorotributylamine	155	0.0133	6.5
Perfluoro-1-methyldecalin	160	0.0143	7.0
Perfluorodimethyldecalin	180	0.0147	7.2

[a] Hildebrand Solubility Parameter

6.5. MIXTURES AND BLENDS

6.5.1. Higher Solvency Azeotropes and Mixtures

The low solvency of PFCs for most nonhalogenated materials has traditionally limited their applicability. However, the formation of PFC/hydrocarbon (HC) azeotropes and PFC/HC mixtures has improved the solvency and subsequently enhanced the applicability of PFCs in numerous industrial processes.

One azeotropic mixture is currently available for evaluation in experimental quantities. The azeotrope L-12862 is composed of 90 wt % PFC and 10 wt % 2,2,4-trimethylpentane. The physical properties of this material are given in Table 6.5. This azeotrope exhibits improved hydrocarbon solubility characteristics and retains the excellent halogenated solubility characteristics of PFCs. Because an azeotrope maintains identical vapor and liquid composition at its boiling point, it will act as a single substance, facilitating its recovery via distillation and containment via condensation.[1]

When more organic solvent power is needed, nonazeotropic mixtures of PFCs and HCs are also available. They are formulated to take advantage of the inerting ability of the PFCs and therefore do not have flash points. Although most hydrocarbons do not exhibit appreciable solubility in PFCs, numerous useful PFC/HC combinations do exist. Some PFC/HC mixtures exhibit complete miscibility and are thus limited only by flash points and flammability. To develop a mixture, the HC solvent(s) can be selected to provide the required solvency properties and substrate compatibility, then an appropriate PFC inerting solvent can be selected. Table 6.6 lists PFC/HC mixtures that have no flash point at the indicated concentrations. Some of these mixtures, or their recipes, are being offered on an experimental basis for evaluation purposes.

Although these materials do not have flash points using standard ASTM test procedures, it is possible that they have flammable limits in air. For example, L-12862 has no flash point, but it does become flammable in air between concentrations of 2.7 and 11.5 vol %. Several common materials exhibit this type of behavior. 1,1,2 Trichloroethylene does not have a flash point and is shipped as a nonflammable material, but shows flammability limits between 12.5

Table 6.5. Azeotrope Physical Properties

Name	Density (g/ml)	Boiling point (°C)	Viscosity (cs)	Surface tension (mN/M)	Phase split temperature (°C)	Flash point
L-12862	1.50	69	0.53	13.42	Cloud −1 Layer −4	None

Table 6.6. Nonflammable Solvent Blends[a]

PFC inerting agent	Hydrocarbon solvent	Volume % PFC
Perfluoropentane	Isopropyl alcohol	50
Perfluoropentane	*n*-Hexane	50
Perfluoropentane	*n*-Heptane	20
Perfluoropentane	Isooctane	50
Perfluoropentane	Hexamethyldisiloxane	50
Perfluoro-*N*-methylmorpholine	*n*-Heptane	22
Perfluorohexane	*n*-Octane	5
Perfluoroheptane	*n*-Octane	6

[a] Nonflammable indicates that no flash point was observed by the ASTM test method D-3278-82 or D-56 below the boiling point of the solvent mixture or below 100°F, whichever is lower (this is the DOT, ANSI, and NFPA definition). The composition of liquid blends can vary from the originally supplied composition during use, owing to the differing vapor pressures of the individual constituents. Care must be taken to avoid preferential loss of PFCs, which would result in flammable mixtures.

and 90 vol % in air.[6] Therefore, caution must be exercised when evaluating the aforementioned azeotropes and mixtures. In addition to explosion limits, the composition of the azeotrope liquids and the PFC/HC mixtures cannot be guaranteed during use, owing to the differing vapor pressures of the individual constituents. Azeotropes that are boiled and used as saturated vapors phase will retain their composition.

6.5.2. Mixtures for Materials Compatibility

HCFCs are viable substitutes for CFCs, but they can have catastrophic effects on some polymeric substrates, owing to increased polarity and solvent strength. To reduce or eliminate substrate attack, PFCs can be combined with HCFCs. PFCs are miscible with most HCFCs, such as HCFC-141b (1,1-dichloro-1-fluoroethane) and HCFC-225 (pentafluorodichloropropane) and therefore can be mixed in any proportion to obtain the desired inerting behavior.

6.5.3. Silicone Solvent

One useful blend currently being employed as a very effective silicone solvent on an industrial scale is a mixture of 80 vol % hydrocarbon heptane and 20 vol % perfluoropentane, called L-12808 (see Table 6.7). L-12808 is useful for applying silicone lubricants to numerous medical devices, such as needles, IV spikes, blood filters, and catheters. This mixture shows no flash point and no explosion limits in air.[6] The presence of the more volatile PFC, relative to the HC,

allows a high concentration of perfluoropentane vapor to exist in the vapor zone above the mixture. This effectively eliminates the flash point of the mixture by precluding the heptane reaching a flammable concentration above the liquid mixture.

Several precautions are necessary to ensure that the perfluoropentane is able to inert the flammability of the heptane. The container in which the material is stored must be kept tightly capped at all times and the container in which the material is used must have a freeboard region above the liquid level. This freeboard region allows the perfluoropentane vapors a volume in which to collect during usage. Also, the more volatile perfluoropentane will escape from the solution more rapidly than the heptane. Therefore, an excess of perfluoropentane must be monitored and maintained in the solution container as a lower phase. As the perfluoropentane evaporates, the excess perfluoropentane will move into the saturated solution to maintain the PFC concentration. Owing to the rapid evaporation of the perfluoropentane, the L-12808 mixture must never be used on a towel or rag, which would provide a large surface for evaporation of the PFC and allow the remaining heptane to become flammable. Because of this, L-12808 is not recommended as a cleaning solvent and all spills of the material should be treated as flammable.

6.6. GAS SOLUBILITY

Another interesting aspect of perfluorinated liquids is their high gas solubility. They can provide highly effective gas transport in chemical reactions and physical processes. In addition, PFCs can be used to absorb or scavenge gases. Table 6.8 shows the solubility of various gases in a perfluorohexane.

Table 6.7. Solubility of Various Silicones In L-12808

Silicone	Maximum silicone solubility (vol %)
ShinEtsu X-22-8100A	20
Wacker Chemie AK 350	17
Dow Corning MDX-360	20
Toshiba THC 9300	6
Dow Corning MDX-4-4759	20
Dow Corning Antifoam	7
Dyna-Glide #1 silicone wax	6

Table 6.8. Gas Solubilities in Perfluorohexane at 1 atm and 25°C

Gas	ml gas/100 ml pefluorohexane	Gas	ml gas/100 ml pefluorohexane
Helium	11	Ethane	282
Argon	65	Ammonia	54
Hydrogen	17	Fluorine	17
Nitrogen	43	Sulfur hexafluoride	957
Oxygen	65	Tetrafluoromethane	129
Carbon dioxide	248	Chlorine	1350
Air	48	Krypton	118
Methane	92		

6.7. ENVIRONMENTAL CONSIDERATIONS

A comprehensive assessment of the environmental impact of any CFC alternative should be made in weighing its relative benefits and liabilities. The magnitude, impact, and disposition of all waste streams should be evaluated. Differences in safety and toxicity need to be considered. Energy requirements may vary substantially, resulting in environmental as well as economic impact.

If handled responsibly, PFCs can be excellent choices to replace ozone-depleting compounds in many demanding, high-performance applications. Perfluorinated liquids are colorless, odorless, essentially nontoxic, and nonflammable. In addition, since they are not precursors to photochemical smog, PFCs are exempt from the U.S. EPAs volatile organic compounds (VOC) definition. Most importantly, these materials do not contain the carbon-bound chlorine or bromine, which can cause ozone depletion.

Minimizing emissions of PFCs is desirable, for both economic as well as environmental reasons. As with most organic compounds that can volatilize into the atmosphere, these materials absorb energy in the IR region of the spectrum. Since PFCs have high stability and long atmospheric lifetimes, they could contribute to global warming, if emitted in large volumes. However, the global warming contribution from the use of PFCs as replacements for ozone-depleting compounds and in other applications has been estimated to be so low as to be indistinguishable from a finding of no warming.* Nevertheless, it is certainly prudent that equipment using PFCs be designed properly to contain the material.

Practically, very low emission rates with PFCs should be achievable for a number of reasons. First, lower loss rates can be obtained because of several beneficial physical properties of PFCs compared to CFCs and other halogenated

* Based on calculations for 3M using a one-dimensional radiative convective model developed by Atmospheric and Engineering Research, Inc.

solvents. The PFCs have lower heats of vaporization, higher vapor densities, and lower diffusivities than CFCs. These properties interact to facilitate easier containment. Second, improvements in containment technology have led to significantly lower emissions rates, which are already being experienced with PFCs, as compared to CFCs, typically ten- to twentyfold less in actual industrial practice. Data from commercial applications employing AVD equipment manufactured by Detrex indicates emissive losses of less than 0.05 lb/(hr × ft^2) have been achieved using current technology. This should result in a decrease in the total global warming impact of PFCs, relative to CFCs, in both the rate of rise and the maximum. Future improvements in containment and recovery technology should make it possible to further reduce emissions. PFCs are readily adsorbed on carbon and the nonpolarity of these molecules permits virtually quantitative thermal desorption and regeneration. Improvements in membrane technology may also be of use in recovering these compounds.[1]

6.8. REFERENCES

1. Mark W. Grenfell, Frank W. Klink, and John G. Owens, Presented at the Nepcon West 1994 Conference, Anaheim, CA, March 4, 1994.
2. DuPont Performance Products Technical Brochure, No. E-92801, 12/88.
3. DuPont Polymers Technical Brochure, No. H-44662.
4. DuPont Polymer Products Department Technical Brochure, No. H-12064.
5. Warren H. Buck and Paul R. Resnick, Presented at the 183rd Meeting of the Electrochemical Society, Honolulu, HI, May 17, 1993.
6. Scott D. Thomas, 3M Internal Memo, September 20, 1993.

7

Fluoropolymer Alloys

Performance Optimization of PVDF Alloys

SHIOW-CHING LIN and
KAROL ARGASINSKI

7.1. INTRODUCTION

The use of polymer blends has been a very important approach in the development of new materials for evolving applications, as it is less costly than developing new polymers. The compatibility of poly(vinylidene fluoride) (PVDF) with various polymers has been comprehensively evaluated and has led to useful applications in coatings and films. Poly(methyl methacrylate) has been the most studied compatible polymer with PVDF owing to cost and performance advantages. Other acrylic polymers such as poly(ethyl methacrylate), poly(methyl acrylate), and poly(ethyl acrylate) have also been found to be compatible with PVDF.[1]

A composition containing at least 70 wt % of PVDF and about 30 wt % of acrylic resin has been recommended as a standard coating formulation. The recommended formulation is designed to provide coatings with optimized physical properties and a resistance to the effects of long-term environmental exposure. In addition to internal research results, a literature search was done to confirm that this composition provides the best balance of optical properties, solvent resistance, hardness, mechanical strength, and weatherability.

SHIOW-CHING LIN and KAROL ARGASINSKI · Ausimont USA, Thorofare, New Jersey 08086.

Fluoropolymers 2: Properties, edited by Hougham *et al.* Plenum Press, New York, 1999.

Mechanisms of resistance to rapamycins

Shile Huang, Peter J. Houghton

Department of Molecular Pharmacology, St. Jude Children's Research Hospital, Memphis, TN 38105-2794

Abstract Rapamycins represent a novel family of anticancer agents, currently including rapamycin and its derivatives, CCI-779 and RAD001. Rapamycins inhibit the function of the mammalian target of rapamycin (mTOR), and potently suppress tumor cell growth by arresting cells in G1 phase or potentially inducing apoptosis of cells, in culture or in xenograft tumor models. However, recent data indicate that genetic mutations or compensatory changes in tumor cells influence the sensitivity of rapamycins. First, mutations of mTOR or FKBP12 prevent rapamycin from binding to mTOR, conferring rapamycin resistance. Second, mutations or defects of mTOR-regulated proteins, including S6K1, 4E-BP1, PP2A-related phosphatases, and $p27^{Kip1}$ also render rapamycin insensitivity. In addition, the status of ATM, p53, PTEN/Akt and 14-3-3 are also associated with rapamycin sensitivity. To better explore the role of rapamycins against tumors, this review will summarize the current knowledge of the mechanism of action of rapamycins, and progress in understanding mechanisms of acquired or intrinsic resistance. © 2002 Elsevier Science Ltd.

Key words: Rapamycin, mTOR, signaling pathways, $p27^{Kip1}$, drug resistance

INTRODUCTION

Rapamycin, a macrocyclic lactone (Fig. 1), is produced by the soil bacteria *Streptomyces hygroscopicus* that was first found on Easter Island in the South Pacific. A group led by Dr. Suren Sehgal, then senior scientist at Ayerst Research Laboratories in Montreal, Canada, firstly isolated rapamycin from the bacteria and identified it as an antifungal agent.[1–3] Soon rapamycin (sirolimus), as a structural analogue of the macrolide antibiotic FK506 (tacrolimus, Prograf®) (Fig. 1), was also found to potently suppress the immune system.[4–7] When rapamycin was sent to the National Cancer Institute (NCI) for testing, surprisingly, the drug also demonstrated potent inhibitory activity against numerous solid tumors.[8–10] Whereas the NCI quickly designated rapamycin as a priority antitumor drug Ayerst abandoned it, because at that time company researchers failed to develop a satisfactory intravenous formulation for use in clinical trials. Also at that time, little was known about the mechanism of action of rapamycin in blocking signal transduction. Not until 1988, after Wyeth and Ayerst merged, did studies of rapamycin resume. While solid data convinced Wyeth-Ayerst to develop rapamycin as an immunosuppressant, the NCI and many other laboratories continued to study the antitumor activity of rapamycin. Rapamycin (Rapamune®), as an immunosuppressive drug, was finally approved by the Food and Drug Administration (FDA) in the USA in September, 1999, and the European Commission in March, 2000, respectively. So far, results from many laboratories have demonstrated that rapamycin, in contrast to FK506, is not only a potent immunosuppressant, but also a potential antitumor agent. Rapamycin can act as a cytostatic, arresting cells in G1 phase or potentially inducing apoptosis in many malignant cells in culture. To date, studies have revealed that rapamycin potently arrests growth of cells derived from rhabdomyosarcoma, neuroblastoma and glioblastoma, small cell lung cancer,[11–17] osteoscarcoma,[18] pancreatic cancer,[19,20] breast and prostate cancer,[21–25] murine melanoma and leukemia, and B-cell lymphoma.[9,24–26]

However, direct use of rapamycin as an anticancer drug is clinically impractical, because of its poor water-solubility and stability in solution. Recently, two rapamycin ester analogues (Fig. 1), CCI-779 [rapamycin-42, 2, 2-bis(hydroxymethyl)-propionic acid] (Wyeth-Ayerst, PA, USA) and RAD001 [everolimus, 40-O-(2-hydroxyethyl)-rapamycin] (Novartis, Basel, Switzerland), with improved pharmaceutical properties have been synthesized and evaluated. CCI-779 is designed for intravenous injection, whereas RAD001 for oral administration. Both have similar antitumor effects as rapamycin,[17,21–23,27–30] and are currently being developed as antitumor agents and undergoing phase I/II clinical trials. So far, preclinical results have revealed that rapamycin and its derivatives (designated here as rapamycins) suppress growth of numerous human tumor cells in vitro, and in some human and murine tumor models in vivo.[11–30] When combined with other chemotherapeutic agents, rapamycins generally show at least additive antitumor activity.[10,12,17,31] Preliminary data from clinical trials have indicated that rapamycins are well tolerated and successfully suppress growth of various human tumors.[32–34] However, increasing evidence has suggested that genetic mutations or compensatory changes in tumor cells may affect the sensitivity of rapamycins. For instance, mutations of the mammalian target of rapamycin (mTOR) or FKBP12 prevent rapamycin from binding to mTOR and confer rapamycin resistance. Mutations or defects of mTOR-controlled downstream effector molecules, such as S6K1, 4E-BP1, PP2A-related phosphatases, and $p27^{Kip1}$, also render rapamycin insensitivity. At least in some systems the status of ATM, p53, PTEN/Akt and 14-3-3 also determines rapamycin sensitivity. This review will summarize the current knowledge of action mechanism of rapamycins, and resistance mechanisms.

MECHANISM OF ACTION OF RAPAMYCINS

Rapamycins represent a novel family of anticancer agents, currently including rapamycin and its derivatives, CCI-779 and RAD001. Rapamycins share a common mechanism of antitumor action. Simply, they inhibit the function of mTOR that links mitogen stimulation to protein synthesis and cell cycle progression, and potently suppress tumor cell growth by arresting cells at G1 phase, potentially inducing apoptosis of cells.

mTOR and its inhibition by rapamycin

The mammalian target of rapamycin, mTOR [also designated FRAP (FKBP12 and rapamycin-associated protein), RAFT1

© 2002 Elsevier Science Ltd. Drug Resistance Updates (2001) 4, 378–391
doi 10.1054/drup.2002.0227, available online at http://www.idealibrary.com on IDEAL®

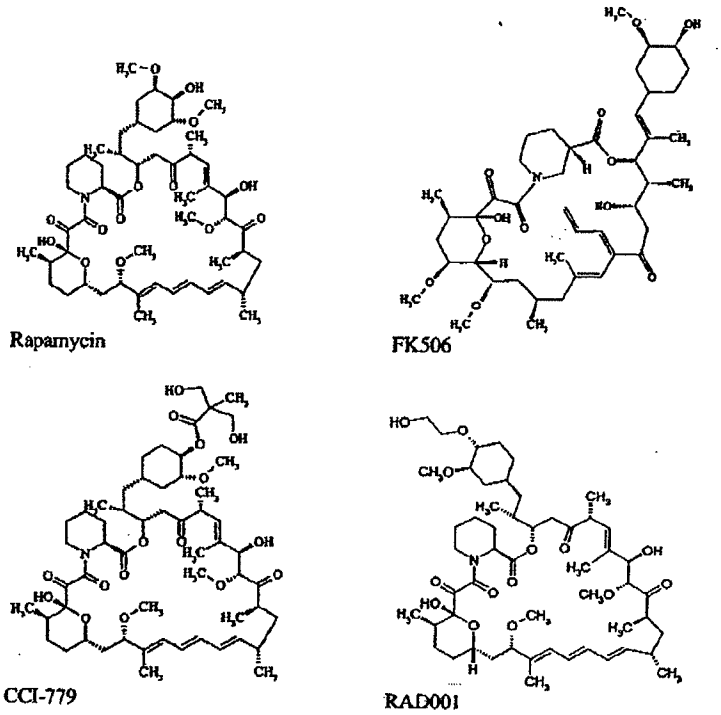

Fig. 1 **Structures of rapamycin, FK506, and two rapamycin analogues in clinical trials, CCI-779 and RAD001.**

(rapamycin and FKBP12 target 1), RAPT1 (rapamycin target 1) or SEP (sirolimus effector protein)), was identified as a 289 kDa serine/threonine kinase from mammalian cells.[35–38] According to Genebank database, TOR proteins are evolutionarily conserved from yeast to human beings in the catalytic domain. In the yeasts, *Saccharomyces cerevisiae* and *Schizosaccharomyces pombe*, two TOR genes, designated TOR1 and TOR2, have been cloned, both sharing 67% homology and encoding ~280 kDa proteins.[39–41] In the fruit fly, *Drosophila melanogaster*, a single TOR orthologue, termed dTOR, has been characterized, sharing 38% identity with TOR2 from *Saccharomyces cerevisiae*.[42,43] Mammalian TOR (mTOR) shares ~45% identity with TOR1 and TOR2 from the yeast *Saccharomyces cerevisiae*, and 56% identity with dTOR in overall sequence.[44,45] Human, mouse and rat mTOR proteins share 95% identity at the amino acid level.[46,47] Structurally, mTOR is composed of a catalytic kinase domain, FRB (FKBP-rapamycin binding) domain and a putative auto-inhibitory domain ("repressor domain") near C-terminus, and up to 20 tandemly repeated HEAT (Huntingtin, EF3, A subunit of PP2A and TOR) motifs at the N-terminus, as well as FAT (FRAP-ATM-TRAPP) and FATC (FAT C-terminus) domains (Fig. 2).[47,48] Since the

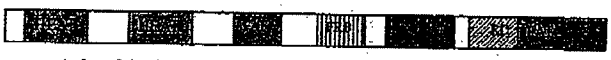

Fig. 2 **Schematic representation of the domains of mTOR. Structural domains of mTOR. HEAT: (huntingtin elongation A subunit TOR) repeats (positions 71–522 and 628–1147); FAT: (FRAP-ATM-TRAPP) domain, which is unique to PIK-related kinases located N-terminal to the FKBP12-rapamycin binding domain (FRB); the role of FAT sequences is less clear, but they are associated with C-terminal FAT (FATC) sequences in mTOR interaction between FAT and FATC domains may facilitate protein binding or act as a structural scaffold; CD: Catalytic domain; RD: regulatory domain.**

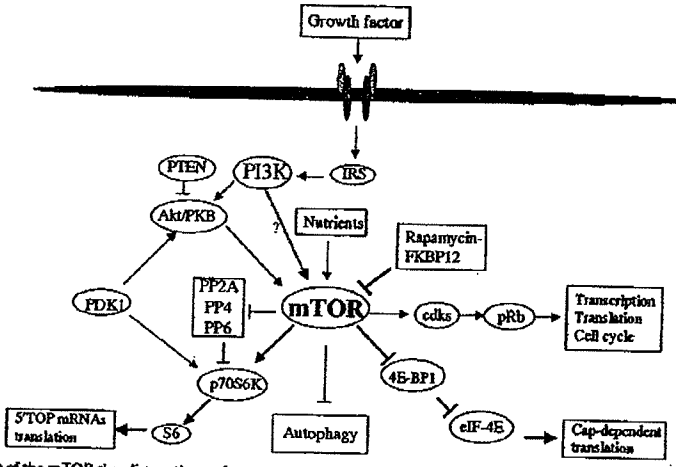

Fig. 3 **Scheme of the mTOR signaling pathway. Arrows represent activation, whereas bars represent inhibition. IRS, insulin receptor substrates; PI3K, phosphatidylinositol 3′ kinase; PIP_2, phosphatidylinositide (4,5)-P_2; PIP_3, phosphatidylinositide (3,4,5)-P_3; PTEN, phosphatase and tensin homologue deleted on chromosome ten; PDK1, phosphoinositide-dependent protein kinase 1; Akt/PKB, protein kinase B; rapamycin-FKBP12, rapamycin-FK506-binding protein 12 complex; mTOR, mammalian target of rapamycin; pRb, retinoblastoma protein; Pol I/II/III, RNA polymerase I/II/III; 4E-BP1, eIF-4E-binding protein 1; eIF-4A/4E/4F/4G/3, eukaryotic initiation factor-4A/4E/4F/4G/3; S6K1, p70 S6 kinase; S6, 40S ribosomal protein; 5′TOP, 5′-terminal oligopyrimidine.**

C-terminus of mTOR is highly homologous to the catalytic domain of phosphatidylinositol 3 kinase (PI3K), mTOR is considered a member of PI3K-related kinase family (designated PIKK), which also includes MEC1, TEL1, RAD3, MEI-41, DNA-PK, ATM, ATR, and TRRAP.[47,49] Both PI3K and, potentially, Akt/PKB lie upstream of mTOR, whereas two translational components, ribosomal p70S6 kinase (S6K1) and eukaryotic translation initiation factor-4E (eIF4E) binding protein 1 (4E-BP1), are the best characterized downstream effector molecules of mTOR (Fig. 3). However, the full spectrum of cellular events controlled by mTOR extends beyond these pathways. Increasing evidence has implicated mTOR as a sensor that integrates extracellular and intracellular events, coordinating growth and proliferation. mTOR may directly or indirectly regulate translation initiation, actin organization, membrane traffic and protein degradation, protein kinase C signaling, ribosome biogenesis and tRNA synthesis, as well as transcription.[47] Recent results suggest that mTOR may also sense cellular ATP levels, suppressing protein synthesis when ATP levels decrease.[50]

Rapamycins are specific inhibitors of mTOR. Although rapamycin and FK506 are both potent immunosuppressive agents, their mechanisms of action are quite different. Both rapamycin and FK506 competitively binds to a M_r 12,000 cytosolic protein termed FK-binding protein (FKBP-12). The FKBP-FK506 complex inhibits calcineurin, preventing dephosphorylation, nuclear translocation of NF-ATp, and activation of interleukin 2 transcription.[46] The FKBP-rapamycin complex binds to the FRB domain of mTOR, resulting in inhibition of the function of mTOR. The specific binding of rapamycin has been confirmed by studies of genetic mutations of mTOR and FKBP12 (see review below for details). Currently, a major unresolved issue is how rapamycin inhibits the function of mTOR. As we know, many small molecule kinase inhibitors reduce the activity of kinases by direct competition for ATP binding, thus preventing ligand-induced autophosphorylation and signaling. However, whether rapamycin or FKBP-rapamycin complex directly inhibits the kinase activity of mTOR is controversial. FKBP-rapamycin complex inhibited autokinase activity of mTOR in vitro at high concentration (500 nM).[51] Rapamycin in vitro also blocked the modest insulin-induced increase of kinase activity of immunoprecipitated mTOR.[52] However, treatment of cells with rapamycin did not alter autophosphorylation level of Ser2481, and had little or no effect on the kinase activity of immunoprecipitated mTOR.[42,45,53] Possibly, mTOR may repress a phosphatase activity associated with downstream targets. Binding of FKBP-rapamycin complex to mTOR may first result in de-repression of this phosphatase, which then dephosphorylates downstream effector molecules, e.g. S6K1[54,55] and p44/42 MAP kinases (our unpublished data).[56] More recently, phosphatidic acid has been identified as a critical component of mTOR signaling, and its binding to mTOR is necessary for activation of mTOR downstream effector molecules.[57] It is also possible that FKBP-rapamycin complex may compete with phosphatidic acid to bind the FRB domain of mTOR, preventing mTOR from activating downstream effectors although without inhibiting mTOR's catalytic activity.[57] Alternatively, mTOR may act as a scaffold

and the FKBP-rapamycin complex presumably disrupts higher order mTOR-protein complexes. Obviously, more studies are required to establish a suitable model for rapamycin action.

Rapamycin-sensitive signaling pathways mediated by mTOR

As mentioned above, 4E-BP1 and S6K1 are the best characterized downstream effector molecules of mTOR (Fig. 3). Both are translational components. 4E-BP1 functions as a suppressor of eIF4E. In response to mitogens, six sites (Thr37, Thr46, Ser65, Thr70, Ser83, and Ser112) of 4E-BP1 (also termed PHAS-I) can be phosphorylated.[58] So far, only mTOR and ATM have been identified to be involved in phosphorylation of 4E-BP1.[59–62] Little is known whether other kinases participate in phosphorylation of 4E-BP1. ATM phosphorylates 4E-BP1 at Ser112,[62] whereas mTOR in vitro selectively phosphorylates 4E-BP1 at two and possibly four Ser/Thr residues (Thr37, Thr46, Thr70 and Ser65) in the N-terminal region.[61,63] 4E-BP1 phosphorylation is a hierarchical process.[61,63–65] Phosphorylation of Thr37/Thr46 is followed by Thr70 phosphorylation, and Ser65 is phosphorylated last.[65] Phosphorylation of Ser65 depends on phosphorylation of all three Thr/Pro sites,[63,64] whereas mutations of Thr37 and/or Thr46 to alanine(s) prevents phosphorylation of Ser65 and Thr70, suggesting that phosphorylation of Thr37 and Thr46 serves as a requisite 'priming' event.[55] Single phosphorylation of above residues is not sufficient to dissociate 4E-BP1 from eIF4E, indicating that a combined phosphorylation of at least Thr37, Thr46, Ser65, and Thr70 in 4E-BP1 is essential to suppress association with eIF4E.[55,66] In the presence of rapamycin, 4E-BP1 becomes hypo-phosphorylated and associates with eIF4E. This prevents binding of eIF4E to the scaffold protein eIF4G and formation of the eIF4F initiation complex required for cap-dependent translation of mRNA. As a result, rapamycin may downregulate mTOR-controlled synthesis of essential proteins involved in cell cycle progression, such as cyclin D1,[67,68] and ornithinine decarboxylase,[69] and survival (c-MYC).[70]

S6K1 is the other well documented downstream target of mTOR. To date, two ribosomal p70S6 kinases have been identified: S6K1 and S6K2, and both can be inhibited by rapamycin.[71,72] S6K1 contains a nuclear localization signal domain at the N-terminus, followed by an acidic domain, a catalytic domain, a regulatory domain, an auto-inhibitory domain and C-terminal domain.[73] Activation of S6K1 is a complex process that involves the interplay between four different domains and at least seven specific sites mediated by multiple upstream kinases.[73] It has been reported that at least 12 sites (Ser17, Thr229, Thr367, Thr371, Thr389, Ser404, Ser411, Ser418, Tr421, Ser424, Ser429, and Thr447) can be phosphorylated in response to serum stimulation.[58] However, the kinases responsible for the phosphorylation of these sites are not fully characterized. Phosphoinositide-dependent protein kinase 1 (PDK1) phosphorylates Thr229 in vitro and in vivo.[74] Atypical PKC isoforms and the Rho family of small G proteins (cdc42 and Rac1) may partially contribute to phosphorylation of S6K1[58], but the specific sites regulated by these kinases remain to be determined. In vitro, mTOR phosphorylates only Thr389 in the regulatory domain.[75–77] However, whether this phosphorylation is directly or indirectly regulated by mTOR is in question, since recent data suggest that mTOR may regulate S6K1 activation by inhibiting phosphatases rather than directly phosphorylating S6K1.[54,73] Similar to 4E-BP1, S6K1 also needs a hierarchical phosphorylation process to be activated. The initial step for S6K1 activation is the phosphorylation of the Ser/Thr-Pro sites in the auto-inhibitory domain, which then cooperates with the N-terminus to allow phosphorylation of Thr389. This presumably disrupts the interaction of the C-terminus with the N-terminus, allowing phosphorylation of Thr229 and resulting in S6K1 activation.[73] As phosphorylation of Thr389 is a primary event for phosphorylation of other sites, in vivo rapamycin may affect phosphorylation of more sites, including Thr229 in the catalytic domain, and Ser404 in the regulatory domain.[75] S6K1 functions to increase translation of mRNA species with 5′ terminal oligopyrimidine (5′TOP) tracts. These mRNAs primarily code for ribosomal proteins and other elements of the translational machinary, such as ribosomal proteins, elongation factors, the poly(A) binding proteins,[72] and IGF-II.[78] Therefore, inhibition of mTOR by rapamycin primarily downregulates translation of 5′TOP-containing mRNAs.

In addition to inhibition of translation of specific mRNAs through 4E-BP1 and S6K1 pathways, rapamycin may also suppress RNA polymerase (Pol) I/II/III-mediated transcription and translation by decrease of mTOR-controlled phosphorylation of retinoblastoma protein (pRb).[66] Furthermore, rapamycin may also inhibit activation of G1 cyclin-dependent kinases (cdks) causing hypophosphorylation of pRb protein, and slow or arrest cell cycle transition from G1 to S-phase.[79] The mechanism by which rapamycin inhibits activity of cdks may be cell type dependent, either by upregulation of cdk inhibitors, or downregulation of cyclins or cdks, or inhibition of association of cyclin-cdks. For example, in T lymphocytes, rapamycin increases the level of cdk inhibitory protein $p27^{Kip1}$ by prevention of its degradation induced by mitogens.[80,81] Involvement of $p27^{Kip1}$ being an effector of rapamycin-induced G1 cell cycle arrest is strengthened by the observation that $p27^{Kip1}$ deficient T lymphocytes or fibroblasts are relatively resistant to rapamycin inhibition of growth.[82] In NIH3T3 cells rapamycin may inhibit the G1 to S transition through inhibition of cdks by decrease of the cyclin D1 mRNA level and protein stability,[68] or delay of the expression of cyclin A.[83] In vascular smooth muscle cells, growth factors elevate the levels of cell cycle proteins, such as cyclins (D1, E, B) and cdks (cdk1 and cdk2), whereas rapamycin blocks the upregulation of these proteins, but not mRNA, and arrests the cells before S phase.[84] In contrast to findings in other cell types, in vascular smooth muscle cells rapamycin does not affect growth factor-induced downregulation of $p27^{Kip1}$.[84] In MG-63 human osteosarcoma cells, rapamycin inhibits cdk activity and cyclin D1-cdk association during early G1.[85] Similarly, in T lymphocytes, rapamycin also blocks activation of cdk1 ($p34^{cdk2}$) and cdk2 ($p33^{cdk2}$) by inhibition of cyclin A expression, and formation of active cyclin A-cdk1/2 complexes and cyclin E-cdk2 complex, resulting in late G1 arrest.[86]

MECHANISMS OF RESISTANCE TO RAPAMYCINS

As observed by Dilling et al.[11] various cell lines exhibit several thousand-fold differences in their intrinsic sensitivity to rapamycin under similar growth conditions. Further studies indicate that the response to rapamycin is different

between cell lines, being either cytostatic or cytotoxic, or cytostatic/cytotoxic.[14–16] The mechanism for this intrinsic resistance is under investigation. However, increasing data have implicated that cells may acquire resistance either with or without mutagenesis. Obviously, the mechanisms of rapamycin resistance are complicated and multiple, some of which have been identified whereas others remain to be determined. Reported mechanisms of rapamycin resistance are summarized below.

Mutations in FKBP12 and mTOR

As aforementioned, rapamycin has a specific mode of action. It cannot directly bind to mTOR. It first has to bind to FKBP-12 in mammalian cells, forming the FKBP-rapamycin complex. This complex then interacts with the FRB domain in mTOR (Fig. 2), and inhibits the function of mTOR. Therefore, during such sequential interactions, either specific mutations in FKBP12 that prevent the formation of FKBP-rapamycin complex, or certain mutations in the FRB domain of mTOR that block binding of FKBP-rapamycin complex to mTOR would finally abrogate the effect of rapamycin on mTOR, causing rapamycin resistance. Such mutations were first found in yeast. For example, *S. cerevisiae* treated with rapamycin irreversibly arrested in the G1 phase. A mutational screen identified rapamycin-resistant alleles with mutations in genes designated TOR1 and TOR2. Strains with mutated to TOR1-1 (Ser1972 → Arg) and TOR2-1 (Ser1975 → Arg), were completely resistant to the growth-inhibitory effect of rapamycin. These resistant alleles encode mutant TOR proteins that lack the ability for FKBP-rapamycin complex binding.[87–92] The results suggest that a conserved serine residue (Ser1972 in TOR1; Ser1975 in TOR2) in yeast TOR proteins is critical for FKBP-rapamycin binding. In mammalian cells, resistance to rapamycin selected after mutagenesis is related to a dominant phenotype also consistent with mutation in the FRB domain of mTOR,[93] that results in decreased affinity for binding of the FKBP-rapamycin complex. Expression of a mutant mTOR (Ser2035 → Ile), having reduced affinity for binding the FKBP-rapamycin complex, confers high level resistance.[14,93,94] Alternatively, in the yeast *S. cerevisiae*, deletion of the RBP1 gene, a homologue of mammalian FKBP-12, resulted in a recessive rapamycin resistance, whereas expression of RBP1 restored rapamycin sensitivity.[87] This observation has been further confirmed by RBP1 disruption experiments using the pathogenic yeast *Candida albicans*, in which the wild-type RBP1/RBP1 parental strain and the rbp1/RBP1 heterozygous mutant were sensitive to rapamycin inhibition, whereas rbp1/rbp1 homozygous mutant was rapamycin resistant.[95] In addition, in *S. cerevisiae* mutation of a specific residue (Tyr89) which is conserved in RBP1 or FKBPs, also resulted in decreased binding of rapamycin and conferred a recessive resistance phenotype.[96] In murine mast cells, two distinct point mutations in FKBP12, one altering a hydrophobic residue within the drug-binding pocket (Trp59 → Leu) and the other changing a charged surface residue (Arg49 → Gln), substantially reduced binding affinity of FKBP12 for rapamycin, rendered rapamycin resistance.[97]

Mutations in S6K1

As described above, S6K1 is a principal downstream effector of mTOR. So far, data have revealed that rapamycin primarily inhibits only phosphorylation of Thr389 in the regulatory domain.[73] However, since phosphorylation of S6K1 is hierarchical with phosphorylation of several other sites dependent on phosphorylation of Thr389,[73] rapamycin in vivo influences phosphorylation of more sites, including Thr229 in the catalytic domain, and Ser404 in the regulatory domain.[75] Therefore, site mutation of Thr389 → Glu abrogates the ability of rapamycin to inhibit S6K1 activation.[72,75] Similarly, substitution of Thr229 by either a neutral amino acid Ala (Thr229 → Ala) or by an acidic amino acid Glu (Thr229 → Glu), renders S6K1 insensitive to rapamycin.[98] In addition, deletion of the 77 N-terminal codons (ΔN77) conferred rapamycin resistance.[99] It turns out that truncation of the first 54 residues of N-terminus (otherwise identical to ΔN77 above) blocked the serum-induced phosphorylation of three rapamycin-sensitive sites, Thr229, Thr389 and Ser404, causing rapamycin insensitivity.[75] Whether this results in resistance to the growth inhibitory effect of rapamycin is less clear, and may be cell context specific.

De-regulation of eIF4E

Besides S6K1, 4E-BP1, the suppressor of eIF4E, has been widely recognized as the other primary downstream effector of mTOR.[55] Recently, our group has found that acquired resistance to rapamycin was associated with decreased levels of 4E-BP1 (Dilling et al. submitted).[100] Briefly, rapamycin-resistant cell lines, Rh30/Rapa10K and C2 clones, were obtained by continuously culturing Rh30 parental cells in the presence of increasing concentrations of rapamycin, without prior mutagenesis. In the absence of selective pressure, resistance was unstable. Within 10 weeks after rapamycin was withdrawn from the medium, resistant clones reverted to being sensitive to growth inhibition of rapamycin. The molecular basis of rapamycin resistance in this case has been investigated. It turns out that in Rh30/Rapa10K and C2 cells, the levels of the suppressor protein 4E-BP1 bound to eIF4E were significantly lower (~10-fold), as were total cellular levels of 4E-BP1. However, mRNA levels of 4E-BP1 were unaltered, indicating post-translational regulation. Further studies indicate that the synthesis of 4E-BP1 did significantly decrease in rapamycin-resistant clones, but whether the steady state level of 4E-BP is also regulated by increased degradation remains to be determined. Thus, the changes in 4E-BP levels are reminiscent of those reported for $p27^{Kip1}$ in BC3H cells.[82] In cells (Rh30/Rapa10-revertant) that reverted to be sensitive to rapamycin, total levels of 4E-BP1 became similar to those in parental cells, and 4E-BP1 bound to eIF4E had similar response to serum starvation and IGF-I stimulation as found in parental cells. In contrast, no significant changes were detected for S6K1 levels or activity between parental and resistant clones. Activation of S6K1 was equally inhibited in parental and rapamycin-resistant clones. Both Rh30/Rapa10K cells and Rh30/Rapa10K-revertant cells exhibited elevated c-MYC levels, and increased anchorage-independent growth, indicating that inhibition of c-MYC translation by rapamycin is not critical in determining rapamycin sensitivity. These data suggest that decrease of 4E-BP1 expression results in de-regulation of eIF4E, conferring rapamycin resistance.

According to the above findings, rapamycin-regulated eIF4E pathway is crucial in inducing growth arrest, and de-regulation of eIF4E may facilitate malignant phenotype. This

is supported by certain clinical observations that de-regulation of the eIF4E pathway does promote tumor progression.[101] In addition to decrease of 4E-BP1 expression, as described above, increased eIF4E levels may also cause de-regulation of eIF4E. In advanced head and neck carcinoma,[102] breast carcinoma[103] and gastrointestinal carcinoma,[104] eIF4E levels are elevated. However, levels of 4E-BP proteins have not been reported in a consistent manner. Potentially, the ratio of 4E-BP:eIF4E may determine whether inhibition of mTOR elicits a biologically significant tumor response. Certainly, intrinsic resistance to rapamycin has been shown in glioblastoma cells and colon adenocarcina that have very low 4E-BP:eIF4E ratios (our unpublished data). In addition, HCT8 colon carcinoma cells are highly resistant to rapamycin (IC_{50} > 10,000 ng/ml). When 4E-BP1 is overexpressed, these cells become sensitive (IC_{50} > 10 ng/ml) to rapamycin (Dilling et al. submitted). However, further studies will be necessary to determine if this ratio has predictive value for drug sensitivity of tumors.

Mutations of PP2A-related phosphatases

So far, several Ser/Thre protein phosphatases, such as PP2A, PP4 and PP6, have been identified as the components of mTOR signaling pathway in mammalian cells.[66] Mammalian PP2A is composed of a common core dimer of a 39 kDa catalytic C-subunit (PP2Ac) and a 65 kDa A-subunit associated with diverse distinct regulatory B-subunits (50~130 kDa). Rapamycin resistance caused by mutations of PP2A-related phosphatases was first studied in yeast. In *S. cerevisiae*, PPH21 and PPH22 encode C-subunits of PP2A (Pph21 and Pph22), whereas TPD3 and CDC55 respectively encode 64 kDa A-subunit and 60 kDa B-subunit. Tap42 is the yeast homologue of mammalian α4, and Sit4 is the yeast homologue of PP6, and the catalytic subunit of a PP2A-related phosphatase in yeast. Early studies in yeast indicate that Tap42 associates with Sit4 and Pph21/22.[105] The function of Tap42 remains to be determined. However, it appears to be a gene essential for cell division and survival. Strains overexpressing isogenic tap42-11 mutants were almost completely resistant to rapamycin.[105] In addition, overexpression of Sit4, but not Pph21, also resulted in weak rapamycin resistance.[105] The mechanism of rapamycin resistance in this case is still unknown. Rapamycin did not decrease Tap42 protein level, but caused dissociation of Tap42 from Sit4 and Pph21/22.[105] Two possibilities accounting for rapamycin resistance were discussed by the authors.[105] First, if Tap42 functioned as a positive regulatory subunit for Sit4 and Pph21/22, in rapamycin-resistant tap42-11 strains, the mutant protein might be stably associated with the phosphatases and maintain a specific phosphatase activity that is insensitive to rapamycin. Second, if phosphatases regulated a specific Tap42 function, in the rapamycin-resistant Tap42-11 mutant, the function of the Tap42-11 protein would be less dependent on the association with the phosphatases, also causing rapamycin resistance.

Similarly, mutations or deletion of either TPD3 (encoding Tpd3, A subunit) or CDC55 (encoding Cdc55, B subunit), which regulate Pph21/22 activity, conferred rapamycin resistance.[106] This is because TPD3 or CDC55 mutants failed to compete with TOR-phosphorylated Tap42 binding to Pph21/22 C-subunit, resulting in increased association of Tap42 with Pph21/22.[106] These findings suggest that Tap42, Sit4 and PP2A might be downstream effectors of TOR proteins. Studies of mammalian cells also indicate that association of α4 with PP2A, PP4, and PP6 is related to rapamycin sensitivity.[107,108] For example, in rapamycin-sensitive Jurkat cells, rapamycin dissociated α4 from PP2Ac, whereas in rapamycin-resistant Raji cells, rapamycin did not affect association of α4 with PP2Ac.[108] Transfection of mouse α4 into Jurkat cells conferred rapamycin resistance,[108] further demonstrating that these PP2A-related phosphatases are novel rapamycin-sensitive targets. Surprisingly, rapamycin inhibits cell proliferation by decreasing PP2A activity through dissociating α4 from PP2Ac,[108] suggesting that PP2A may positively regulate cell proliferation under certain conditions. However, other studies[109] did not demonstrate rapamycin-induced dissociation of α4 from PP2A or PP6. Thus, at this time the significance of α4 remains controversial.

Defective regulation of $p27^{Kip1}$

$p27^{Kip1}$, a cdk inhibitor, is downregulated in serum stimulated cells. Prevention of mitogen-stimulated downregulation of $p27^{Kip1}$ level by rapamycin suggests that $p27^{Kip1}$ is involved in the antiproliferative activity of rapamycin.[80,81] Rapamycin resistance linked to defective regulation of $p27^{Kip1}$ has been described.[82] BC3H1 is a rapamycin-sensitive murine myogenic cell line. Prolonged culture of BC3H1 cells in the presence of rapamycin without any induced mutagenesis resulted in rapamycin-resistant clones, RR-1 (selected with 0.1 μM rapamycin) and RR-3 (selected with 1 μM rapamycin). Compared with parental BC3H1 cells, two RR cell lines showed no impairment of inhibitory pathway, as determined by either Western blot analysis or direct activity assay. However, RR cells exhibited abnormally low $p27^{Kip1}$ protein, but no decrease in mRNA level. Further studies revealed that this was due to a high rate of ubiquitin-independent degradation. Importantly, $p27^{Kip1}$ in RR cells could not be regulated any more, since it was neither reduced in response to serum nor augmented in response to rapamycin. As a result, pRb phosphorylation was blocked by rapamycin in parental MC3H1 cells but not in RR cells. Rapamycin inhibited proliferation or ^{3}H-thymidine incorporation to a greater extent in parental BC3H1 cells than in RR cells. Partial resistance to antiproliferative activity of rapamycin was further found in $p27^{-/-}$ mouse embryo fibroblasts and $p27^{-/-}$ splenic T lymphocytes, indicating that there might exist p27-dependent and -independent pathways that determine rapamycin sensitivity. Whether other cdk inhibitors are involved in rapamycin sensitivity remains to be determined.

Mutations of ATM

ATM (ataxia telangiectasia, mutated) is a 370-kDa protein kinase, which is encoded by the gene mutated in the human genetic disorder ataxia-telangiectasia (A-T) characterized by neuronal degeneration, immunodeficiency, sterility, genomic instability, cancer predisposition, and radiation sensitivity.[110] Like mTOR, the C-terminal sequence of ATM is highly homologous to the catalytic domain of PI3-kinase.[49,111] Recent studies have shown rapamycin resistance in A-T cells.[112] When lymphoblastoid cells were exposed to rapamycin and viability was determined by dye (trypan blue) exclusion at 72 h post-treatment. Three A-T cell lines were significantly more

resistant to cell killing by rapamycin than controls at 10 ng/ml or 20 ng/ml, but more sensitive to the PI3-kinase inhibitor wortmannin.[112] Mutations at certain residues of ATM did not determine rapamycin resistance or wortmannin sensitivity, since three A-T cell lines exhibited different mutations in the ATM. Other findings support rapamycin resistance in A-T cells. Rapamycin inhibited cell cycle progression from G1 to S phase in control cells, but failed to prevent cell cycle progression in A-T cells.[112] Consistently, rapamycin decreased phosphorylation of and cdk2 kinase activity in control cells, but did not affect activation of both and cdk2 in A-T cells. Although ATM is not the direct target of FKBP-rapamycin complex, a number of other proteins (50-200 kDa) were augmented in their binding to the rapamycin-FKBP complex in the A-T cell lines.[112] The authors thus proposed that increased resistance to rapamycin in A-T cell lines could be due to alteration in the level of a target protein as a consequence of loss of ATM. In contrast, early passage murine embryo fibroblasts derived from $ATM^{-/-}$ mice are not resistant to rapamycin (Germain, Houghton, unpublished data). Thus the null phenotype is distinct from the ATM mutant cells. As the ATM cells have genetic instability it is possible that the reported resistance to rapamycin is a consequence of additional mutations and not related directly to defects in ATM signaling.

Mutations of 14-3-3

The 14-3-3 proteins are a highly conserved family of scaffolding and adaptor proteins, with a molecular mass ranging from 27 to 32 kDa, that bind to Ser/Thre-phosphorylated residues in a context specific manner.[113] They participate in cell cycle control, signal transduction and apoptosis by regulating protein-protein interactions, subcellular localization of proteins, and enzyme activity.[114] In the yeast *S. cerevisiae*, BMH1 and BMH2 are the two homologues of the 14-3-3 family and act as multicopy suppressors of the growth-inhibitory phenotype caused by rapamycin.[115] Overexpression of BMH1 or BMH2 alone conferred rapamycin resistance, whereas disruption of BMH1 and/or BMH2 sensitized the yeast to rapamycin.[115] Interestingly, overexpression of three human 14-3-3 isoforms (β, τ and η) in the yeast also conferred rapamycin resistance. The results suggest that the rapamycin-sensitive function of 14-3-3 proteins is conserved from yeast to human and is isoform-independent. In addition, single or double mutations of BMH1 (Leu232→Ser and Gly55→Asp) resulted in dominant rapamycin resistance. The mechanism by which 14-3-3 proteins cause rapamycin resistance is not known. Since the yeast TOR proteins lack consensus sites for 14-3-3 binding, TOR proteins could not directly associate with Bmh1p or Bmh2p. Thus, direct interference by Bmh1p and Bmh2p with FKBP-rapamycin binding to Tor1p and Tor2p in the budding yeast may be excluded. Additional studies are necessary to address whether a direct interaction between 14-3-3 proteins and a downstream effector of TOR proteins, or perhaps other mechanisms confer rapamycin resistance.

Mutations of p53

p53 is a tumor suppressor and transcription factor that has been found to be mutated in ~50% of human cancers.[116,117] The function of p53 depends on cell type and developmental stage.[118] In response to genotoxic damage, such as exposure to chemotherapeutic agents, γ-irradiation, or UV irradiation, p53 is upregulated, which may result in either G1 cell cycle arrest and DNA repair, or apoptosis.[117] Recent studies indicate that p53 status may also determine rapamycin sensitivity.[16] The results demonstrate that the responses of malignant and normal cells to rapamycin are qualitatively different. When treated with rapamycin, p53-wild type normal cells arrest in G1 phase and maintain viability. In contrast, when cultured under autocrine conditions (serum-free), p53 mutant rhabdomyosarcoma cells (Rh30) accumulate in G1 phase and undergo apoptosis. More than 90% of cells demonstrating morphologic signs of apoptosis were bromodeoxyuridine-labeled, suggesting that the cells died in S phase. Thus, rapamycin-induced death appears to be a consequence of continued cell cycle progression. The molecular mechanism by which rapamycin induces p53-independent apoptosis is under investigation.

The protective role of p53 has been further examined using Ad-p53 (adenovirus expressing p53) infected Rh30. Infection of Rh30 cells with Ad-p53 restored p53-mediated G1 checkpoint. More than 86% of cells arrested in G1 phase and remained viable when exposed to rapamycin (Fig. 4).[16] Similarly, in the presence of rapamycin, $p53^{-/-}$ MEFs cells continue cell cycle progression, and become apoptotic, whereas $p53^{+/+}$ MEFs cells arrest in G1 and remain viable. These results support the notion that p53 senses some consequence of mTOR inhibition and reinforces G1 arrest. Although the mechanism of p53 protection against rapamycin-induced apoptosis remains to be determined, the above data suggest a mechanistic basis for tumor-selective cytotoxicity of rapamycins.

Loss of PTEN and/or activation of Akt

PTEN (phosphatase and tensin-homologue deleted on chromosome ten), also designated MMAC1 (mutated in multiple advanced cancers), is a dual-specificity protein phosphatase, and functions as a major negative regulator of the PI3-kinase/Akt signaling pathway.[119–121] Loss of PTEN by genetic deletion or mutation occurs in as many as 50% of all solid human tumors,[122] resulting in hyperphosphorylation or activation of Akt. mTOR has been reported to be directly phosphorylated by Akt,[52,123] although this is still controversial.[40,53] Therefore, in principle, phosphorylated Akt might activate mTOR-dependent pathways thus form the basis for rapamycin or CCI-779 hypersensitivity of PTEN deficient or mutant cells. This view-point has been supported by recent findings.[22,23,29,30] For example, PTEN loss in tumor cells or in MEFs cells elevated activity of S6K1 and phosphorylation of 4E-BP1, two major downstream effectors of mTOR. Either loss of PTEN or activation of Akt resulted in an increased sensitivity to CCI-779 in a panel of brain, prostate, breast cancer cell lines and in MEFs cells.[22,23,29,30] However, there are exceptions where loss of PTEN is not associated with hypersensitivity to CCI-779. The association of PTEN deficiency and sensitivity to rapamycin are supported by the activity of CCI-779 against the growth of human tumors implanted in athymic nude mice (Fig. 5).[22,23,30] Consistently, most CCI-779 resistant tumor cells had a low or moderate level of activated Akt.[22] Moreover, $PTEN^{+/-}$ mice developed spontaneous multifocal complex atypical hyperplasia in the uterine secretory epithelium that progresses to neoplastic transformation, and

Drug Resistance Updates (2001) 4, 378–391

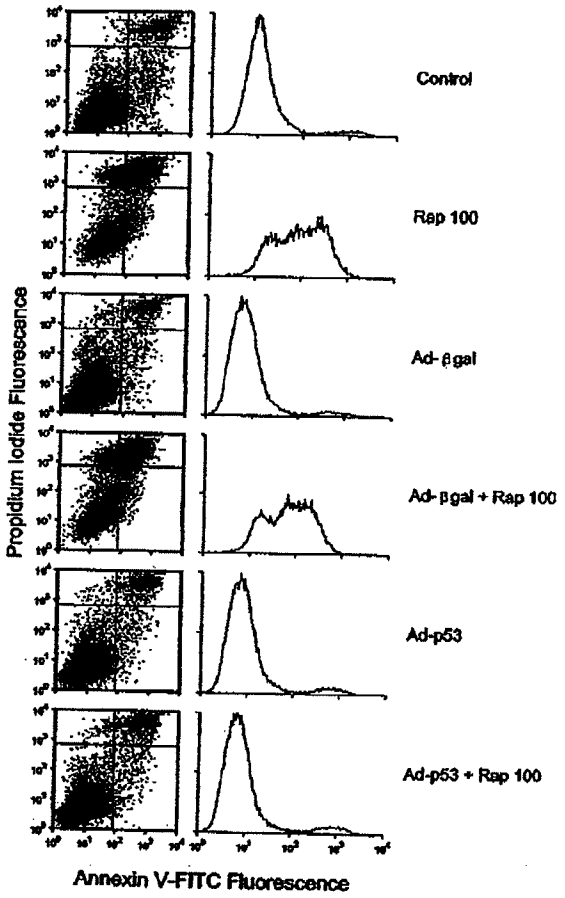

Fig. 4 **Protective effect of the tumor suppressor p53 on rapamycin-induced apoptosis. Rh30 rhabdomyosarcoma cells were infected with either Ad-p53 or Ad-β-gal adenovirus (MOI of 1). After 24 h medium was replaced with serum-free N2E, and cells were grown for a further six days without or with rapamycin (100 ng/ml). Cells were harvested and apoptosis determined by quantitative FACs analysis (ApoAlert). Left panels show dual staining for propidium iodide uptake and annexin V-FITC. Right panels show corresponding distribution of annexin V-FITC staining in populations of cells. (Adapted from Huang et al.[18] with permission)**

neoplasia of the chromaffin cells of the adrenal medulla.[29] Transformed PTEN$^{+/-}$ tumor cells exhibited increased levels of phosphorylated Akt and activated S6K1. Although CCI-779 had no effect on Akt activation, as anticipated, it normalized S6K1 activity, reducing neoplastic proliferation and tumor size.[29] In long-term (~10 weeks) trials, seven PTEN$^{+/-}$ mice administered with CCI-779 appeared more active, and by the end of the study, all were alive, while 3/13 animals died of uterine or gastrointestinal tumors in the control (mock-treated and untreated) groups.[29]

Prevention of apoptosis by insulin-like growth factor I (IGF-I)

Induction of apoptosis by rapamycin is specifically due to inhibition of mTOR signaling. Rhabdomyosarcoma cells (Rh1 and Rh30) engineered to stably express a mutant form of mTOR

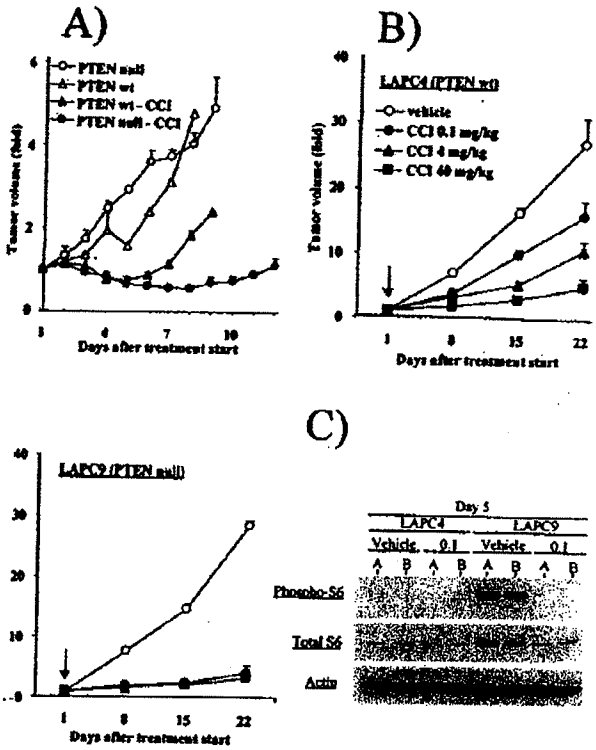

Fig. 5 PTEN null cells have enhanced sensitivity to mTOR inhibition in vivo. (A) PTEN$^{+/+}$ or PTEN$^{-/-}$ ES cells were injected s.c. into nude mice at a dose of 5×10^6 cells per mouse ($n = 20$). When tumor volume reached 200 mm^3, mice were randomized to treatment with vehicle or 40 mg/kg CCI-779. The fold change in tumor volume in response to treatment was plotted. (B) Single-cell suspensions of LAPC-4 or LAPC-9 prostate cancer xenografts were injected s.c. into male SCID mice ($n = 80$) at a dose of 10^6 cells per mouse. When tumors became palpable, mice were randomized (arrow) to treatment with vehicle, 0.1 mg/kg, 4 mg/kg or 40 mg/kg CCI-779. The fold change in tumor volume from two independent experiments is plotted. (C) Tumors were harvested from mice after five days of treatemnt with vehicle or 0.1 mg/kg CCI-779 and lysed by boiling in 2% SDS buffer. Immunoblots were performed by using antibodies for phosphorylated S6 (Ser-235/236), total S6, and actin. (Adapted from Neshat et al.[17] with permission)

resistant to rapamycin (Ser2035→Ile) are highly resistant (>3000-fold) to both growth inhibition and apoptosis induced by rapamycin. Exogenous IGF-I or insulin protected from apoptosis, without re-activating ribosomal S6K1.[14,15] Of interest, EGF, PDGF, and VEGF, like IGF-I or insulin, each of which activates Akt and MAP kinase (Erk1/2) pathways in the cells examined, failed to significantly protect against rapamycin-induced apoptosis (our unpublished data).[124] Overexpression of dominant negative Ras (Ras/N-17) in Rh1 cells, or treatment of cells with either farnesyltransferase inhibitor SCH66336 or MEK1 inhibitor PD98059, did not alter the protection of IGF-I against rapamycin-induced apoptosis. Similarly, overexpression of dominant negative Akt (Lys179→Met) also failed to change the protective effect of IGF-I against rapamycin-induced cell death. Moreover, even in the presence of both the PI3K inhibitors wortmannin or LY294002 and MEK1 inhibitor PD98059, IGF-I continued to prevent cells from rapamycin-induced apoptosis. Accordingly, the results suggest that signals arising from the Ras/Erk1/2 or the PI3K/Akt pathways either independently or collectively do not contribute to the protective effects of IGF-I against rapamycin-induced apoptosis. Further studies are obviously necessary, since understanding the signaling pathways involved in IGF-I protection will be important to develop new approaches to therapy aimed at converting the cytostatic response to rapamycin into a cytotoxic response in tumor cells.

SUMMARY

In summary, rapamycins act as specific inhibitors of mTOR, a central integrator in signal transduction. Inhibition of mTOR by rapamycin may down-regulate S6K1/eIF4E dependent translation, or block cdk-mediated G1/S cell cycle transition, resulting in inhibition of cell growth and proliferation, as well as apoptosis of some tumor cell lines. Preclinical studies, together with preliminary data from clinical trials, have demonstrated that rapamycins are promising novel antitumor agents. However, increasing evidence have implicated that resistance to rapamycins may occur by multiple mechanisms. Decreased binding of rapamycins to the target mTOR, because of mutations in FKBP-12 and mTOR, may cause resistance to rapamycins. Mutations or defects of downstream effector molecules of mTOR, such as S6K1, 4E-BP1/eIF4E, PP2A-related phosphatases, and $p27^{Kip1}$, also protect cells from inhibition by rapamycins. Furthermore, the status of ATM, p53, PTEN/Akt and 14-3-3 are other factors that may determine sensitivity to rapamycins. It appears that stable resistance to rapamycins can be gained by genetic mutations, whereas unstable resistance can be acquired by epigenic changes, such as decreased expression of 4E-BPs. Whether genetic mutations of p53 and PTEN really sensitize cells to rapamycins requires to be confirmed clinically. It is anticipated that rapamycins, as antitumor agents, may be more effective when clinically used in combination, either with conventional cytotoxic agents, or with inhibitors of other signaling pathways.

Acknowledgements

Supported in part by USPHS awards CA77776, CA23099 and CA28765 (Cancer Center Support Grant) from the National Cancer Institute, through a grant from Wyeth-Ayerst Company, and American, Lebanese, Syrian Associated Charities (ALSAC).

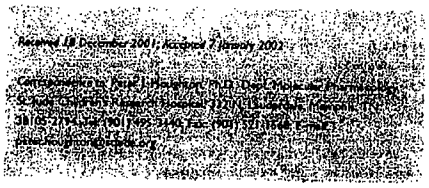

Received 18 December 2001; Accepted 7 January 2002

Correspondence to: Peter J. Houghton, Ph.D., Department of Molecular Pharmacology, St. Jude Children's Research Hospital, 332 N. Lauderdale, Memphis, TN 38105-2794, USA. Tel: (901) 495-3346; Fax: (901) 521-1648; E-mail: peter.houghton@stjude.org

References

1. Vezina C, Kudelski A, Sehgal SN. Rapamycin (AY-22,989), a new antifungal antibiotic. I. Taxonomy of the producing streptomycete and isolation of the active principle. J Antibiot (Tokyo) 1975; 28: 721–726.
2. Sehgal SN, Baker H, Vezina C. Rapamycin (AY-22,989), a new antifungal antibiotic. II. Fermentation, isolation and characterization. J Antibiot (Tokyo) 1975; 28: 727–732.
3. Sehgal SN. Rapamune (RAPA, *rapamycin*, sirolimus): mechanism of action immunosuppressive effect results from blockade of signal transduction and inhibition of cell cycle progression. Clin Biochem 1998; 31: 335–340.
4. Calne RY, Collier DS, Lim S, Pollard SG, Samaan A, White DJ, Thiru S. Rapamycin for immunosuppression in organ allografting. Lancet 1989; 2: 227.
5. Schreiber SL. Chemistry and biology of the immunophilins and their immunosuppressive ligands. Science 1991; 251: 283–287.
6. Pohanka E. New immunosuppressive drugs: an update. Curr Opin Urol 2001; 11: 143–151.
7. Saunders RN, Metcalfe MS, Nicholson ML. Rapamycin in transplantation: a review of the evidence. Kidney Int 2001; 59: 3–16.
8. Douros J, Suffness M. New antitumor substances of natural origin. Cancer Treat Rev 1981; 8: 63–87.
9. Houchens DP, Ovejera AA, Riblet SM, Slagel DE. Human brain tumor xenografts in nude mice as a chemotherapy model. Eur J Cancer Clin Oncol 1983; 19: 799–805.
10. Eng CP, Sehgal SN, Vezina C. Activity of rapamycin (AY-22,989) against transplanted tumors. J Antibiot (Tokyo) 1984; 37: 1231–1237.
11. Dilling MB, Dias P, Shapiro DN, Germain GS, Johnson RK, Houghton PJ. Rapamycin selectively inhibits the growth of childhood rhabdomyosarcoma cells through inhibition of signaling via the type I insulin-like growth factor receptor. Cancer Res 1994; 54: 903–907.
12. Shi Y, Frankel A, Radvanyi LG, Penn LZ, Miller RG, Mills GB. Rapamycin enhances apoptosis and increases sensitivity to cisplatin in vitro. Cancer Res 1995; 55: 1982–1988.
13. Seufferlein T, Rozengurt E. Rapamycin inhibits constitutive $p70^{s6k}$ phosphorylation, cell proliferation, and colony formation in small cell lung cancer cells. Cancer Res 1996; 56: 3895–3897.
14. Hosoi H, Dilling MB, Liu LN, Danks MK, Shikata T, Sekulic A, Abraham RT, Lawrence JC Jr, Houghton PJ. Studies on the mechanism of resistance to rapamycin in human cancer cells. Mol Pharmacol 1998; 54: 815–824.
15. Hosoi H, Dilling MB, Shikata T, Liu LN, Shu L, Ashmun RA, Germain GS, Abraham RT, Houghton PJ. Rapamycin causes poorly reversible inhibition of mTOR and induces p53-independent apoptosis in human rhabdomyosarcoma cells. Cancer Res 1999; 59: 886–894.
16. Huang S, Liu LN, Hosoi H, Dilling MB, Shikata T, Houghton PJ. $p53/p21^{CIP1}$ cooperate in enforcing rapamycin-induced G1 arrest and determine the cellular response to rapamycin. Cancer Res 2001; 61: 3373–3381.
17. Geoerger B, Kerr K, Tang CB, Fung KM, Powell B, Sutton LN, Phillips PC, Janss AJ. Antitumor activity of the rapamycin analog CCI-779 in human primitive neuroectodermal tumor/medulloblastoma models as single agent and in combination chemotherapy. Cancer Res 2001; 61: 1527–1532.
18. Ogawa T, Tokuda M, Tomizawa K, Matsui H, Itano T, Konishi R, Nagahata S, Hatase O. Osteoblastic differentiation is enhanced by rapamycin in rat osteoblast-like osteosarcoma (ROS 17/2.8) cells. Biochem Biophys Res Commun 1998; 249: 226–230.
19. Grewe M, Gansauge F, Schmid RM, Adler G, Seufferlein T. Regulation of cell growth and cyclin D1 expression by the constitutively active FRAP-S6K1 pathway in human pancreatic cancer cells. Cancer Res 1999; 59: 3581–3587.
20. Shah SA, Potter MW, Ricciardi R, Perugini RA, Callery MP. Frap-S6K1 signaling is required for pancreatic cancer cell proliferation. J Surg Res 2001; 97: 123–130.
21. Gibbons JJ, Discafani C, Peterson R, Hernandez R, Skotnicki J, Frost P. The effect of CCI-779, a novel macrolide anti-tumor agent,

on the growth of human tumor cells in vitro and in nude mouse xenografts in vivo. Proc Am Assoc Cancer Res 1999; 40: 301.
22. Yu K, Zhang W, Lucas J, Toral-Barza L, Peterson R, Skotnicki J, Frost P, Gibbons J. Deregulated PI3K/AKT/TOR pathway in PTEN-deficient tumor cells correlates with an increased growth inhibition sensitivity to a TOR kinase inhibitor CCI-779. Proc Am Assoc Cancer Res 2001; 42: 802.
23. Yu K, Toral-Barza L, Discafani C, Zhang WG, Skotnicki J, Frost P, Gibbons JJ. mTOR, a novel target in breast cancer: the effect of CCI-779, an mTOR inhibitor, in preclinical models of breast cancer. Endocr Relat Cancer 2001; 8: 249–258.
24. Holtsch T, Martin R, Hohman RJ. The effect of the immunophilin ligands rapamycin and FK506 on proliferation of mast cells and other hematopoietic cell lines. Mol Biol Cell 1992; 3: 981–987.
25. Gottschalk AR, Boise LH, Thompson CB, Quintans J. Identification of immunosuppressant-induced apoptosis in a murine B-cell line and its prevention by bcl-x but not bcl-2. Proc Natl Acad Sci USA 1994; 91: 7350–7354.
26. Muthukkumar S, Ramesh TM, Bondada S. Rapamycin, a potent immunosuppressive drug, causes programmed cell death in B lymphoma cells. Transplantation 1995; 60: 264–270.
27. Dudkin L, Dilling MB, Cheshire PJ, Harwood FC, Hollingshead M, Arbuck SG, Travis R, Sausville EA, Houghton PJ. Biochemical correlates of mTOR inhibition by the rapamycin ester CCI-779 and tumor growth inhibition. Clin Cancer Res 2001; 7: 1758–1764.
28. Beuvink I, O'Reilly T, Zumstein S, Zilbermann F, Sedrani R, Kozma S, Thomas G, Lane HA. Antitumor activity of RAD001, an orally active rapamycin derivative. Proc Am Assoc Cancer Res 2001; 42: 366.
29. Neshat MS, Mellinghoff IK, Tran C, Stiles B, Thomas G, Petersen R, Frost P, Gibbons JJ, Wu H, Sawyers CL. Enhanced sensitivity of PTEN-deficient tumors to inhibition of FRAP/mTOR. Proc Natl Acad Sci USA 2001; 98: 10314–10319.
30. Podsypanina K, Lee RT, Politis C, Hennessy I, Crane A, Puc J, Neshat M, Wang H, Yang L, Gibbons J, Frost P, Dreisbach V, Blenis J, Gaciong Z, Fisher P, Sawyers C, Hedrick-Ellenson L, Parsons R. An inhibitor of mTOR reduces neoplasia and normalizes p70/56 kinase activity in Pten$^{+/-}$ mice. Proc Natl Acad Sci USA 2001; 98: 10320–10325.
31. Ishitsuka T, Sakata N, Johnston GL, Gelfand EW, Terada N. Rapamycin potentiates dexamethasone-induced apoptosis and inhibits JNK activity in lymphoblastoid cells. Biochem Biophys Res Commun 1997; 230: 386–391.
32. Raymond E, Alexandre J, Dapenbrock H, Vago AN, Faivre S, Lahn-Randak A, Materman E, Boni J, Abbas S, Angevin E, Escudier B, Armand JP. CCI-779, an ester analogue of rapamycin that interacts with PTEN/PI3 kinase pathways: a phase I study utilizing a weekly intravenous schedule. Clin Cancer Res 2000; 6: 4549S.
33. Hidalgo M, Rowinsky E, Erlichman C, Drengler R, Marshall B, Adjei A, Hammond L, Galanis E, Edwards T, Burton J, Boni J, Dukart G, Tolcher A, Dukart G, Buckner J. Phase I and pharmacological study of CCI-779, a cell cycle inhibitor. Clin Cancer Res 2000; 6: 4548S.
34. Hidalgo M, Rowinsky EK. The rapamycin-sensitive signal transduction pathway as a target for cancer therapy. Oncogene 2000; 19: 6680–6686.
35. Brown EJ, Albers MW, Shin TB, Ichikawa K, Keith CT, Lane WS, Schreiber SL. A mammalian protein targeted by G1-arresting rapamycin-receptor complex. Nature 1994; 369: 756–758.
36. Chiu MI, Katz H, Berlin V. RAPT1, a mammalian homolog of yeast Tor, interacts with the FKBP12/rapamycin complex. Proc Natl Acad Sci USA 1994; 91: 12574–12578.
37. Sabatini DM, Erdjument-Bromage H, Lui M, Tempst P, Snyder SH. RAFT1: a mammalian protein that binds to FKBP12 in a rapamycin-dependent fashion and is homologous to yeast TORs. Cell 1994; 78: 35–43.
38. Sabers CJ, Martin MM, Brunn GJ, Williams JM, Dumont FJ, Wiederrecht G, Abraham RT. Isolation of a protein target of the FKBP12-rapamycin complex in mammalian cells. J Biol Chem 1995; 270: 815–822.
39. Kunz J, Henriquez R, Schneider U, Deuter-Reinhard M, Movva NR, Hall MN. Target of rapamycin in yeast, TOR2, is an essential phosphatidylinositol kinase homolog required for G1 progression. Cell 1993; 73: 585–596.
40. Helliwell SB, Wagner P, Kunz J, Deuter-Reinhard M, Henriquez R, Hall MN. TOR1 and TOR2 are structurally and functionally similar but not identical phosphatidylinositol kinase homologues in yeast. Mol Biol Cell 1994; 5: 105–118.
41. Weisman R, Choder M. The fission yeast TOR homolog, tor1+, is required for the response to starvation and other stresses via a conserved serine. J Biol Chem 2001; 276: 7027–7032.
42. Oldham S, Montagne J, Radimerski T, Thomas G, Hafen E. Genetic and biochemical characterization of dTOR, the *Drosophila* homolog of the target of rapamycin. Genes Dev 2000; 14: 2689–2694.
43. Zhang H, Stallock JP, Ng JC, Reinhard C, Neufeld TP. Regulation of cellular growth by the *Drosophila* target of rapamycin dTOR. Genes Dev 2000; 14: 2712–2724.
44. Abraham RT. Mammalian target of rapamycin: immunosuppressive drugs uncover a novel pathway of cytokine receptor signaling. Curr Opin Immunol 1998; 10: 330–336.
45. Raught B, Gingras AC, Sonenberg N. The target of rapamycin (TOR) proteins. Proc Natl Acad Sci USA 2001; 98: 7037–7044.
46. Abraham RT, Wiederrecht GJ. Immunopharmacology of rapamycin. Annu Rev Immunol 1996; 14: 483–510.
47. Schmelzle T, Hall MN. TOR, a central controller of cell growth. Cell 2000; 103: 253–262.
48. Sekulic A, Hudson CC, Homme JL, Yin P, Otterness DM, Karnitz LM, Abraham RT. A direct linkage between the phosphoinositide 3-kinase-AKT signaling pathway and the mammalian target of rapamycin in mitogen-stimulated and transformed cells. Cancer Res.2000; 60: 3504–3513.
49. Abraham RT. Cell cycle checkpoint signaling through the ATM and ATR kinases. Genes Dev 2001; 15: 2177–2196.
50. Dennis PB, Jaeschke A, Saitoh M, Fowler B, Kozma SC, Thomas G. Mammalian TOR: a homeostatic ATP sensor. Science 2001; 294: 1102–1105.
51. Brown EJ, Beal PA, Keith CT, Chen J, Shin TB, Schreiber SL. Control of p70 s6 kinase by kinase activity of FRAP *in vivo*. Nature 1995; 377: 441–446.
52. Scott PH, Brunn GJ, Kohn AD, Roth RA, Lawrence JC Jr. Evidence of insulin-stimulated phosphorylation and activation of the mammalian target of rapamycin mediated by a protein kinase B signaling pathway. Proc Natl Acad Sci USA 1998; 95: 7772–7777.
53. Peterson RT, Beal PA, Comb MJ, Schreiber SL. FKBP12-rapamycin-associated protein (FRAP) autophosphorylates at serine 2481 under translationally repressive conditions. J Biol Chem 2000; 275: 7416–7423.
54. Peterson RT, Desai BN, Hardwick JS, Schreiber SL. Protein phosphatase 2A interacts with the 70-kDa S6 kinase and is

activated by inhibition of FKBP12-rapamycin associated protein. Proc Natl Acad Sci USA 1999; 96: 4438–4442.
55. Gingras AC, Raught B, Sonenberg N. Regulation of translation initiation by FRAP/mTOR. Genes Dev 2001; 15: 807–826.
56. Houghton PJ, Harwood FC, Ververka KA, Sharif M. Rapid activation of ERK1/2 in response to type I insulin-like growth factor is dependent on the rapamycin-target, mTOR kinase. Proc Am Assoc Cancer Res 2001; 42: 679.
57. Fang Y, Vilella-Bach M, Bachmann R, Flanigan A, Chen J. Phosphatidic acid-mediated mitogenic activation of mTOR signaling. Science 2001; 294: 1942–1945.
58. Shah OJ, Anthony JC, Kimball SR, Jefferson LS. 4E-BP1 and translational integration sites for nutritional and hormonal information in muscle. Am J Physiol Endocrinol Metab 2000; 279: E715–729.
59. Brunn GJ, Hudson CC, Sekulic A, Williams JM, Hosoi H, Houghton PJ, Lawrence JC Jr, Abraham RT. Phosphorylation of the translational repressor PHAS-I by the mammalian target of rapamycin. Science 1997; 277: 99–101.
60. Hara K, Yonezawa K, Kozlowski MT, Sugimoto T, Andrabi K, Weng QP, Kasuga M, Nishimoto I, Avruch J. Regulation of eIF-4E BP1 phosphorylation by mTOR. J Biol Chem 1997; 272: 26457–26463.
61. Gingras AC, Gygi SP, Raught B, Polakiewicz RD, Abraham RT, Hoekstra MF, Aebersold R, Sonenberg N. Regulation of 4E-BP1 phosphorylation: a novel two-step mechanism. Genes Dev 1999; 13: 1422–1437.
62. Yang DQ, Kastan MB. Participation of ATM in insulin signalling through phosphorylation of eIF-4E-binding protein 1. Nat Cell Biol 2000; 2: 893–898.
63. Mothe-Satney I, Brunn GJ, McMahon LP, Capaldo CT, Abraham RT, Lawrence JC Jr. Mammalian target of rapamycin-dependent phosphorylation of PHAS-I in four (S/T)P sites detected by phospho-specific antibodies. J Biol Chem 2000; 275: 33836–33843.
64. Mothe-Satney I, Yang D, Fadden P, Haystead TA, Lawrence JC Jr. Multiple mechanisms control phosphorylation of PHAS-I in five (S/T)P sites that govern translational repression. Mol Cell Biol 2000; 20: 3558–3567.
65. Gingras AC, Raught B, Gygi SP, Niedzwiecka A, Miron M, Burley SK, Polakiewicz RD, Wyslouch-Cieszynska A, Aebersold R, Sonenberg N. Hierarchical phosphorylation of the translation inhibitor 4E-BP1. Genes Dev 2001; 15: 2852–2864.
66. Dennis PB, Fumagalli S, Thomas G. Target of rapamycin (TOR): balancing the opposing forces of protein synthesis and degradation. Curr Opin Genet Dev 1999; 9: 49–54.
67. Rosenwald IB, Kaspar R, Rousseau D, Gehrke L, Leboulch P, Chen JJ, Schmidt EV, Sonenberg N, London IM. Eukaryotic translation initiation factor 4E regulates expression of cyclin D1 at transcriptional and post-transcriptional levels. J Biol Chem 1995; 270: 21176–21180.
68. Hashemolhosseini S, Nagamine Y, Morley SJ, Desrivieres S, Mercep L, Ferrari S. Rapamycin inhibition of the G1 to S transition is mediated by effects on cyclin D1 mRNA and protein stability. J Biol Chem 1998; 273: 14424–14429.
69. Shantz LM, Pegg AE. Overproduction of ornithine decarboxylase caused by relief of translational repression is associated with neoplastic transformation. Cancer Res 1994; 54: 2313–2316.
70. Zimmer SG, DeBenedetti A, Graff JR. Translational control of malignancy: the mRNA cap-binding protein, eIF-4E, as a central regulator of tumor formation, growth, invasion and metastasis. Anticancer Res 2000; 20: 1343–1351.
71. Jefferies HB, Fumagalli S, Dennis PB, Reinhard C, Pearson RB, Thomas G. Rapamycin suppresses 5'TOP mRNA translation through inhibition of S6K1. EMBO J 1997; 16: 3693–3704.
72. Shima H, Pende M, Chen Y, Fumagalli S, Thomas G, Kozma SC. Disruption of the S6K1/p85^{S6K} gene reveals a small mouse phenotype and a new functional S6 kinase. EMBO J 1998; 17: 6649–6659.
73. Volarevic S, Thomas G. Role of S6 phosphorylation and S6 kinase in cell growth. Prog Nucleic Acid Res Mol Biol 2001; 65: 101–127.
74. Pullen N, Dennis PB, Andjelkovic M, Dufner A, Kozma SC, Hemmings BA, Thomas G. Phosphorylation and activation of S6K1 by PDK1. Science 1998; 279: 707–710.
75. Dennis PB, Pullen N, Kozma SC, Thomas G. The principal rapamycin-sensitive S6K1 phosphorylation sites, T-229 and T-389, are differentially regulated by rapamycin-insensitive kinase kinases. Mol Cell Biol 1996; 16: 6242–6451.
76. Burnett PE, Barrow RK, Cohen NA, Snyder SH, Sabatini DM. RAFT1 phosphorylation of the translational regulators p70 S6 kinase and 4E-BP1. Proc Natl Acad Sci USA 1998; 95: 1432–1437.
77. von Manteuffel SR, Dennis PB, Pullen N, Gingras AC, Sonenberg N, Thomas G. The insulin-induced signalling pathway leading to S6 and initiation factor 4E binding protein 1 phosphorylation bifurcates at a rapamycin-sensitive point immediately upstream of S6K1. Mol Cell Biol 1997; 17: 5426–5436.
78. Nielsen FC, Ostergaard L, Nielsen J, Christiansen J. Growth-dependent translation of IGF-II mRNA by a rapamycin-sensitive pathway. Nature 1995; 377: 358–362.
79. Marx SO, Jayaraman T, Go LO, Marks AR. Rapamycin-FKBP inhibits cell cycle regulators of proliferation in vascular smooth muscle cells. Circ Res 1995; 76: 412–417.
80. Nourse J, Firpo E, Flanagan WM, Coats S, Polyak K, Lee MH, Massague J, Crabtree GR, Roberts JM. Interleukin-2-mediated elimination of the p27^{Kip1} cyclin-dependent kinase inhibitor prevented by rapamycin. Nature 1994; 372: 570–573.
81. Barata JT, Cardoso AA, Nadler LM, Boussiotis VA. Interleukin-7 promotes survival and cell cycle progression of T-cell acute lymphoblastic leukemia cells by down-regulating the cyclin-dependent kinase inhibitor p27^{Kip1}. Blood 2001; 98: 1524–1531.
82. Luo Y, Marx SO, Kiyokawa H, Koff A, Massague J, Marks AR. Rapamycin resistance tied to defective regulation of p27^{Kip1}. Mol Cell Biol 1996; 16: 6744–6751.
83. Chen Y, Knudsen ES, Wang JY. The RB/p107/p130 phosphorylation pathway is not inhibited in rapamycin-induced G1-prolongation of NIH3T3 cells. Oncogene 1996; 13: 1765–1771.
84. Braun-Dullaeus RC, Mann MJ, Seay U, Zhang L, von Der Leyen HE, Morris RE, Dzau VJ. Cell cycle protein expression in vascular smooth muscle cells *in vitro* and *in vivo* is regulated through phosphatidylinositol 3-kinase and mammalian target of rapamycin. Arterioscler Thromb Vasc Biol 2001; 21: 1152–1158.
85. Albers MW, Williams RT, Brown EJ, Tanaka A, Hall FL, Schreiber SL. FKBP-rapamycin inhibits a cyclin-dependent kinase activity and a cyclin D1-Cdk association in early G1 of an osteosarcoma cell line. J Biol Chem 1993; 268: 22825–22829.
86. Morice WG, Wiederrecht G, Brunn GJ, Siekierka JJ, Abraham RT. Rapamycin inhibition of interleukin-2-dependent p33^{cdk2} and p34^{cdc2} kinase activation in T lymphocytes. J Biol Chem 1993; 268: 22737–22745.

87. Heitman J, Movva NR, Hall MN. Targets for cell cycle arrest by the immunosuppressant rapamycin in yeast. Science 1991; 253: 905–909.
88. Cafferkey R, Young PR, McLaughlin MM, Bergsma DJ, Koltin Y, Sathe GM, Faucette L, Eng WK, Johnson RK, Livi GP. Dominant missense mutations in a novel yeast protein related to mammalian phosphatidylinositol 3-kinase and VPS34 abrogate rapamycin cytotoxicity. Mol Cell Biol 1993; 13: 6012–6023.
89. Stan R, McLaughlin MM, Cafferkey R, Johnson RK, Rosenberg M, Livi GP. Interaction between FKBP12-rapamycin and TOR involves a conserved serine residue. J Biol Chem 1994; 269: 32027–32030.
90. Cardenas ME, Heitman J. FKBP12-rapamycin target TOR2 is a vacuolar protein with an associated phosphatidylinositol-4 kinase activity. EMBO J 1995; 14: 5892–5907.
91. Lorenz MC, Heitman J. TOR mutations confer rapamycin resistance by preventing interaction with FKBP12-rapamycin. J Biol Chem. 1995; 270: 27531–27537.
92. Freeman K, Livi GP. Missense mutations at the FKBP12-rapamycin-binding site of TOR1. Gene. 1996; 172: 143–147.
93. Dumont FJ, Staruch MJ, Grammer T, Blenis J, Kastner CA, Rupprecht KM. Dominant mutations confer resistance to the immunosuppressant, rapamycin, in variants of a T cell lymphoma. Cell Immunol 1995; 163: 70–79.
94. Chen J, Zheng XF, Brown EJ, Schreiber SL. Identification of an 11-kDa FKBP12-rapamycin-binding domain within the 289-kDa FKBP12-rapamycin-associated protein and characterization of a critical serine residue. Proc Natl Acad Sci USA 1995; 92: 4947–4951.
95. Cruz MC, Goldstein AL, Blankenship J, Del Poeta M, Perfect JR, McCusker JH, Bennani YL, Cardenas ME, Heitman J. Rapamycin and Less Immunosuppressive Analogs Are Toxic to *Candida albicans* and *Cryptococcus neoformans* via FKBP12-Dependent Inhibition of TOR. Antimicrob Agents Chemother 2001; 45: 3162–3170.
96. Koser PL, Eng WK, Bossard MJ, McLaughlin MM, Cafferkey R, Sathe GM, Faucette L, Levy MA, Johnson RK, Bergsma DJ, Livi GP. The tyrosine89 residue of yeast FKBP12 is required for rapamycin binding. Gene 1993; 129: 159–165.
97. Fruman DA, Wood MA, Gjertson CK, Katz HR, Burakoff SJ, Bierer BE. FK506 binding protein 12 mediates sensitivity to both FK506 and rapamycin in murine mast cells. Eur J Immunol 1995; 25: 563–571.
98. Sugiyama H, Papst P, Gelfand EW, Terada N. p70 S6 kinase sensitivity to rapamycin is eliminated by amino acid substitution of Thr229. J Immunol 1996; 157: 656–660.
99. Mahalingam M, Templeton DJ. Constitutive activation of S6 kinase by deletion of amino-terminal autoinhibitory and rapamycin sensitivity domains. Mol Cell Biol 1996; 16: 405–413.
100. Dilling MB, Germain GS, Houghton PJ. Acquired resistance to rapamycin is mediated by altered regulation of the 4E-BP/eIF-4E pathway. Proc Am Assoc Cancer Res 2000; 41: 804.
101. De Benedetti A, Harris AL. eIF4E expression in tumors: its possible role in progression of malignancies. Int J Biochem Cell Biol 1999; 31: 59–72.
102. Nathan CA, Franklin S, Abreo FW, Nassar R, De Benedetti A, Glass J. Analysis of surgical margins with the molecular marker eIF4E: a prognostic factor in patients with head and neck cancer. J Clin Oncol 1999; 17: 2909–2914.
103. Li BD, Liu L, Dawson M, De Benedetti A. Overexpression of eukaryotic initiation factor 4E (eIF4E) in breast carcinoma. Cancer 1997; 79: 2385–2390.
104. Martin ME, Perez MI, Redondo C, Alvarez MI, Salinas M, Fando JL. 4E binding protein 1 expression is inversely correlated to the progression of gastrointestinal cancers. Int J Biochem Cell Biol 2000; 32: 633–642.
105. Di Como CJ, Arndt KT. Nutrients, via the Tor proteins, stimulate the association of Tap42 with type 2A phosphatases. Genes Dev 1996; 10: 1904–1916.
106. Jiang Y, Broach JR. Tor proteins and protein phosphatase 2A reciprocally regulate Tap42 in controlling cell growth in yeast. EMBO J 1999; 18: 2782–2792.
107. Murata K, Wu J, Brautigan DL. B cell receptor-associated protein alpha4 displays rapamycin-sensitive binding directly to the catalytic subunit of protein phosphatase 2A. Proc Natl Acad Sci USA 1997; 94: 10624–10629.
108. Inui S, Sanjo H, Maeda K, Yamamoto H, Miyamoto E, Sakaguchi N. Ig receptor binding protein 1 (alpha4) is associated with a rapamycin-sensitive signal transduction in lymphocytes through direct binding to the catalytic subunit of protein phosphatase 2A. Blood 1998; 92: 539–546.
109. Chen J, Peterson RT, Schreiber SL. α4 associates with protein phosphatases 2A, 4, and 6. Biochem Biophys Res Commun 1998; 247: 827–832.
110. Shiloh Y, Kastan MB. ATM: genome stability, neuronal development, and cancer cross paths. Adv Cancer Res 2001; 83: 209–254.
111. Savitsky K, Bar-Shira A, Gilad S, Rotman G, Ziv Y, Vanagaite L, Tagle DA, Smith S, Uziel T, Sfez S, Ashkenazi M, Pecker I, Frydman M, Harnik R, Patanjali SR, Simmons A, Clines GA, Sartiel A, Gatti RA, Chessa L, Sanal O, Lavin MF, Jaspers NGJ, Taylor AMR, Arlett CF, Miki T, Weissman SM, Lovett M, Collins FS, Shiloh Y. A single ataxia telangiectasia gene with a product similar to PI-3 kinase. Science 1995; 268:1749–1753.
112. Beamish H, Williams R, Chen P, Khanna KK, Hobson K, Watters D, Shiloh Y, Lavin M. Rapamycin resistance in ataxia-telangiectasia. Oncogene 1996; 13: 963–970.
113. Tzivion G, Shen YH, Zhu J. 14-3-3 proteins; bringing new definitions to scaffolding. Oncogene 2001; 20: 6331–6338.
114. van Hemert MJ, Steensma HY, van Heusden GP. 14-3-3 proteins: key regulators of cell division, signalling and apoptosis. Bioessays 2001; 23: 936–946.
115. Bertram PG, Zeng C, Thorson J, Shaw AS, Zheng XF. The 14-3-3 proteins positively regulate rapamycin-sensitive signaling. Curr Biol 1998; 8: 1259–1267.
116. Hollstein M, Sidransky D, Vogelstein B, Harris CC. p53 mutations in human cancers. Science 1991; 253: 49–53.
117. Levine AJ. p53, the cellular gatekeeper for growth and division. Cell 1997; 88: 323–331.
118. Sionov RV, Haupt Y. The cellular response to p53: the decision between life and death. Oncogene. 1999; 18: 6145–6157.
119. Cantley LC, Neel BG. New insights into tumor suppression: PTEN suppresses tumor formation by restraining the phosphoinositide 3-kinase/AKT pathway. Proc Natl Acad Sci USA 1999; 96: 4240–4245.
120. Stambolic V, Suzuki A, de la Pompa JL, Brothers GM, Mirtsos C, Sasaki T, Ruland J, Penninger JM, Siderovski DP, Mak TW. Negative regulation of PKB/Akt-dependent cell survival by the tumor suppressor PTEN. Cell 1998; 95: 29–39.

121. Wu X, Senechal K, Neshat MS, Whang YE, Sawyers CL. The PTEN/MMAC1 tumor suppressor phosphatase functions as a negative regulator of the phosphoinositide 3-kinase/Akt pathway. Proc Natl Acad Sci USA 1998; 95: 15587–15591.
122. Simpson L, Parsons R. PTEN: life as a tumor suppressor. Exp Cell Res 2001; 264: 29–41.
123. Nave BT, Ouwens M, Withers DJ, Alessi DR, Shepherd PR. Mammalian target of rapamycin is a direct target for protein kinase B: identification of a convergence point for opposing effects of insulin and amino-acid deficiency on protein translation. Biochem J 1999; 344: 427–431.
124. Thimmaiah KN, Veverka KA, Patel DH, Houghton PJ. Protection against rapamycin induced apoptosis by type I insulin-like growth factor is independent of Erk1/2 activity. Proc Am Assoc Cancer Res 2001; 42: 801.